

The differential rotation of stars

L L Kitchatinov

DOI: 10.1070/PU2005v048n05ABEH002099

Contents

1. Introduction	449
2. Observational background	450
2.1 The Sun; 2.2 Stars	
3. The origin of differential rotation	451
3.1 The role of turbulence; 3.2 Meridional circulation; 3.3 Convective heat transport	
4. Mean-field effects of turbulence	455
4.1 Quasilinear approximation; 4.2 The Λ -effect; 4.3 Effective viscosities; 4.4 Effective thermal conductivities	
5. The models	460
5.1 Preliminaries; 5.2 Mean-field models; 5.3 Findings of mean-field models; 5.4 Numerical experiments	
6. Prospects	465
References	466

Abstract. Astronomical observations of recent years have substantially extended our knowledge of the rotation of stars. Helioseismology has found out that the equator-to-pole decline in the angular velocity observed on the solar surface traces down to the deep interior of the Sun. New information has been gained regarding the dependence of the rotational nonuniformities on the angular velocity and mass of the star. These achievements have prompted the development of the theory of differential rotation, which is the focal point of this review. Nonuniform rotation results from the interaction of turbulent convection with rotation. The investigation into the turbulent mechanisms of angular-momentum transport has reached a level at which the obtained results can serve as the basis for developing quantitative models of stellar rotation. Such models contain virtually no free parameters but closely reproduce the helioseismological data on the internal rotation of the Sun. The theoretical predictions on the differential rotation of the stars agree with observations. A brief discussion is held here on the relation between the magnetic activity of stars and the nonuniformity of their rotation and on prospects for further development of the theory.

1. Introduction

Nearly all cosmic objects rotate. They interact weakly with ambient matter and other objects and, as a rule, preserve a substantial part of the angular momentum that they had at the time of their origin. This statement applies, in particular, to stars. Although our proximate star — the Sun — has lost

more than 90% of its original angular momentum over the 4.6 billion years of its life, it still has a conspicuous angular velocity, and the complete axial rotation of the Sun takes slightly less than a month.

A noteworthy feature of the solar rotation is its non-uniformity. The angular velocity is latitude-dependent; it decreases from the equator to the poles by about 30%. Such a rotational state is termed differential rotation. To all appearances, other solar-type stars also rotate nonuniformly. Differential rotation has commanded investigators' attention over many decades. Besides the interest in its origin, studies of differential rotation are also stimulated by its possible key role in the magnetic activity of stars [1, 2]. The 11-year solar cycle, flares, and sunspots on the solar surface are related to differential rotation (which was, apropos, discovered by sunspot observations about a century and a half ago [3], although the earliest evidence was found long before [4]).

Interest in differential rotation has quickened in recent years for various reasons. First, progress in helioseismology [5, 6] has allowed investigating the rotational state of the solar interior. The measured frequencies of global oscillations have provided information for determining the angular-velocity distribution not only over the surface of the Sun but also in its interior [7, 8]. Second, the Doppler–Zeeman imaging technique [9] has allowed tracing the revolution of starspots and measuring the nonuniformity of rotation, as was once done for the Sun. At present, the number of stars whose differential rotation has been determined in this way amounts to several dozen [10]. Third, the theory has already reached a certain degree of completeness, as evidenced by the existence of quantitative models of differential rotation that include individual features of some stars. Theory reproduces the internal rotation of the Sun well, in good agreement with helioseismological data, and observations confirm the theoretical predictions for stars. To all appearances, our current understanding of the physics of differential rotation is basically adequate.

L L Kitchatinov Institute of Solar–Terrestrial Physics Siberian Division, Russian Academy of Sciences,
ul. Lermontova 126, 664033 Irkutsk, Russian Federation
Tel. (7-3952) 27 89 31. Fax (7-3952) 51 16 75
E-mail: kit@iszf.irk.ru

Received 27 October 2004, revised 28 December 2004
Uspekhi Fizicheskikh Nauk 175 (5) 475–494 (2005)
Translated by A V Getling; edited by A M Semikhatov

But this in no way means that this area of knowledge passes into the state of ‘dead science’. The acquisition of new data on time variations in stellar rotation (so-called torsional oscillations), on the relationship between the rotation and magnetic activity, and on the particular patterns of rotation in binary systems is now in progress. The available hydrodynamic theory of stellar rotation should become the basis for the development of the magnetohydrodynamics of large-scale stellar fields. Some steps on this road have already been made.

This review is mainly dedicated to the theory of differential rotation of stars. However, as is often the case in astrophysics, observational data are of paramount importance for theory. For this reason, the observational results most important for the considered subject are also presented. Magnetic effects on differential rotation are discussed only briefly.

2. Observational background

2.1 The Sun

The observed distribution of the angular velocity Ω over the solar surface is commonly represented as

$$\Omega = \Omega_0(1 - b \cos^2 \vartheta - c \cos^4 \vartheta), \quad (1)$$

where Ω_0 is the angular velocity at the equator, ϑ is the colatitude — the polar angle measured from the rotational axis in the corresponding spherical coordinate system, and b and c are dimensionless numerical coefficients that specify the degree of rotational nonuniformity.

Direct measurements of the rotational velocity based on Doppler shifts of spectral lines appear to be the most reliable determinations. They yield $\Omega_0 = 2.87 \times 10^{-6} \text{ rad s}^{-1}$, $b = 0.12$, and $c = 0.17$ [11]. Before the advent of spectral techniques, profile (1) was inferred from the revolution of sunspots. The most widely known result obtained in this way is that of Newton and Nunn [12]: $\Omega_0 = 2.90 \times 10^{-6} \text{ rad s}^{-1}$, $b = 0.19$; the coefficient c was not determined, because sunspots are only observed at relatively low latitudes.

The history of solar observations is now repeating itself for stars, and investigators use information on the motion of starspots to determine the differential rotation. It makes sense to compare the results obtained using this method with spectral measurements, which could give an idea of the accuracy of measuring the differential rotation of stars. We make such a comparison in Fig. 1.

The distribution of the rotational velocity inside the Sun is known from helioseismology [7, 8]. Figure 2 shows the rotational frequency as a function of the relative radius $x = r/R_\odot$ for some latitudes. Our attention is attracted by the rapid decrease of the rotational nonuniformity with depth at x slightly exceeding 0.7. This value of the relative radius corresponds to the base of the convection zone. As the theory of the internal structure of stars tells us, the outer layers of the Sun are involved in turbulent convection. The convection shell is underlain by the so-called radiative core, which is stably (subadiabatically) stratified and where, in all likelihood, no conspicuous mixing of matter occurs. The base of the convection zone is located at $x \simeq 0.73$ [13]. It can be seen from Fig. 2 that the rotational nonuniformity extends throughout the whole convection zone but dies out rapidly with depth in the radiative zone. This fact gives an important hint to the theory and agrees with the basic theoretical concept that differential rotation is maintained by convection.

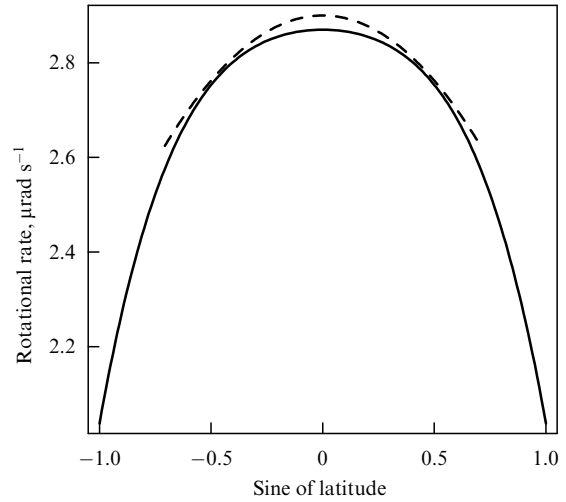


Figure 1. Rotation of the solar surface determined from Doppler measurements [11] (solid curve) and from sunspot rotation [12] (dashed curve).

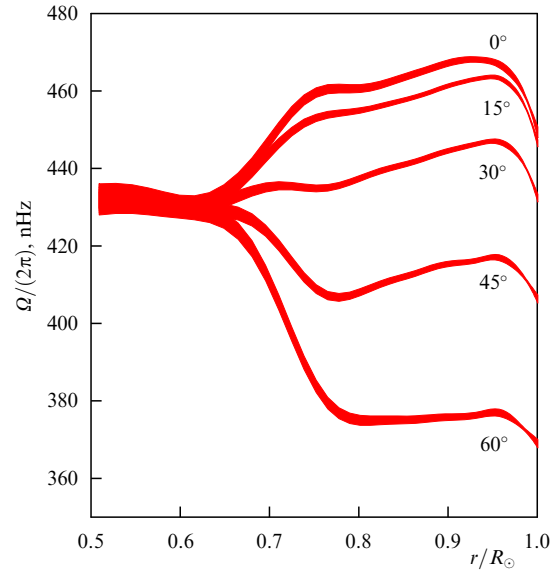


Figure 2. Angular velocity as a function of the relative radius according to the results of the GONG helioseismological project [8]. The individual curves are labeled by the corresponding latitude values.

Except the angular-velocity distribution itself, some other observable quantities — such as the meridional flow or the temperature difference between the poles and the equator — bear relation to the theory of differential rotation. The point is that we cannot determine the angular-velocity distribution alone without simultaneously finding a number of other characteristics related to the nonuniform rotation. Some of them can be inferred from observations. Nevertheless, we postpone the discussion of such observations to the stage at which their connection to our main subject is elucidated.

We note that the representation of the nonuniform rotation in form (1) is not always convenient. Decompositions in terms of the associated Legendre polynomials

$$\Omega = \Omega_0 \sum_{n=1}^N \frac{\omega_n}{\sin \vartheta} P_{2n-1}^1(\cos \vartheta) \quad (2)$$

have some advantages, especially in analyzing time variations of the differential rotation. This is because only the first term of expansion (2) has a finite angular momentum, while all other terms correspond to zero angular momentum. Therefore, if time variations in ω_1 are observed, this means that the surface layers exchange their angular momentum with deeper layers. Obviously, there is the following correspondence between Eqns (1) and (2): $\omega_1 = 1 - b/5 - 3c/35$, $\omega_2 = -2b/15 - 4c/45$, and $\omega_3 = -8c/315$.

2.2 Stars

The rotational nonuniformity of stars can hardly be inferred from observations, because stars appear as point sources of radiation even when observed using the most powerful telescopes. For a long time, indirect techniques were used to measure the differential rotation, and the accuracy of these techniques was difficult to estimate.

The situation changed radically with the advent of the Doppler imaging method [14]. Even before this method received its present-day name, it had been applied to rapidly rotating stars with nonuniform surface distributions of their chemical compositions [15–17]. This technique permits one to map thermal nonuniformities on the surface of a star and trace their temporal changes (the further development of this method, which makes it possible to determine the distribution of the magnetic field over the surface of the star, came to be known as the Doppler–Zeeman imaging). Thus, the differential rotation can be determined from the motion of starspots, in the same manner as this was previously done for the Sun. The basic ideas of this technique are outlined in review [9] and described in more detail in the references therein.

This method derives its name from the Doppler effect, on which it is based. The rotation of the star results in a Doppler broadening of spectral lines. If some area (spot) emits radiation differently from the remainder of the star's surface, the profile of a line is perturbed by this area. As the spot passes over the disk of the star, this disturbance moves from the short-wavelength to the long-wavelength portion of the profile, as shown in Fig. 3. The spatial scale of this displacement increases with the decrease in the latitude of the spot. In this way, the latitudes of the spots can be determined

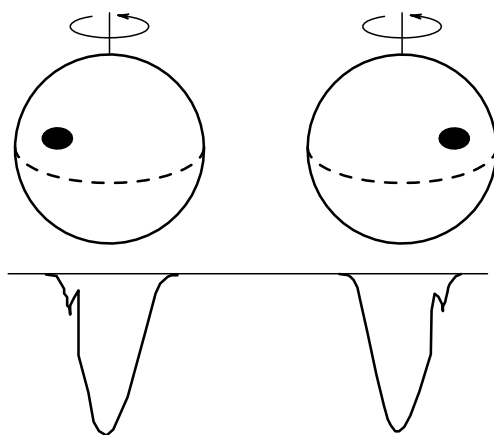


Figure 3. Illustration for the Doppler imaging technique. As the starspot passes from the eastern to the western part of the stellar disk, the spot-related feature in the profile of the (absorption) spectral line moves from the range of relatively short wavelengths to that of relatively long wavelengths.

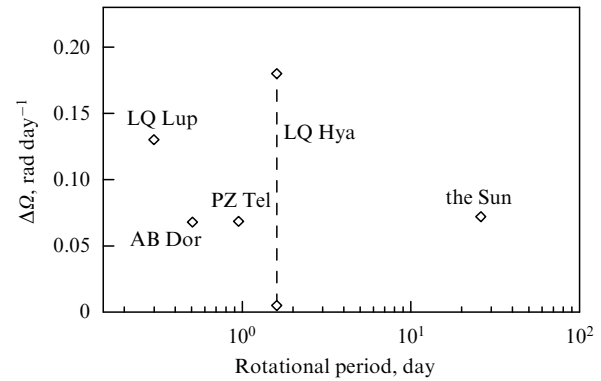


Figure 4. Differential rotation for stars of nearly solar masses but rotating at various rates. AB Dor [18], PZ Tel [20], and LQ Hya [21] are young main-sequence stars. The differential rotation of LQ Hya experiences strong time variations. LQ Lup has not yet reached the main sequence [22].

and their revolution can be traced. The faster the rotation of the star, the better this method works. An equatorial speed of about 15 km s^{-1} is considered a minimum at which the method can be employed (we note for comparison that the equatorial rotational speed of the Sun is about 2 km s^{-1}).

Even the first determination of the differential rotation based on the Doppler imaging method, which was carried out for AB Doradus, a star of the southern celestial hemisphere, yielded interesting results [18]. This star is similar to the Sun in terms of both its mass and chemical composition, but it is younger than the Sun and rotates with a period of about 0.51 days. It was found that the magnitude of the rotational speed nonuniformity, $\Delta\Omega$, for the infant Sun was nearly the same as for the present-day Sun. By now, the differential rotation has been measured for several dozen stars (see, e.g., [10, 19]). Some results of such measurements, which refer to stars of nearly solar masses, are given in Fig. 4. It can be seen that the absolute magnitude of the differential rotation changes little even if the rotational rate changes by almost two orders of magnitude.

The results of Doppler imaging measurements of differential rotation for solar-type stars are systematized by Barnes et al. [23]. They show that, given the spectral class (or mass) of a star, the quantity $\Delta\Omega$ depends weakly on (and, possibly, slightly increases with) the rotational velocity. However, a considerable mass dependence is present. The rotation of stars is more uniform for smaller masses, i.e., for later spectral classes. This agrees well with theoretical predictions [24, 25].

3. The origin of differential rotation

3.1 The role of turbulence

Several hypotheses have been put forward over the long history of the theory of differential rotation. Only one of them has proved its vitality, viz., the idea that rotation becomes nonuniform due to the interaction of convection with global rotation. The convective turbulence in a rotating medium is affected by the Coriolis force. The back reaction disturbs the rotation, rendering it nonuniform. This idea was first formulated by Lebedinskii [26].

To produce differential rotation, the turbulence must transfer angular momentum. This can be inferred from the

equation of motion

$$\frac{\partial \mathbf{v}}{\partial t} + (\mathbf{v} \cdot \nabla) \mathbf{v} + \frac{1}{\rho} \nabla P = \frac{1}{\rho} \nabla \cdot \sigma(\mathbf{v}),$$

$$\sigma_{ij}(\mathbf{v}) = \rho \nu \left(\nabla_i v_j + \nabla_j v_i - \frac{2}{3} \delta_{ij} \operatorname{div} \mathbf{v} \right), \quad (3)$$

where \mathbf{v} is the hydrodynamic velocity, ρ is the density, P is the pressure, σ is the viscous-stress tensor, and ν is the viscosity. Normally, the effects of turbulence are taken into account using the methods of statistical fluid mechanics [27]. The velocity field and other physical fields are divided into a fluctuating and a mean component,

$$\mathbf{v} = \mathbf{u} + \mathbf{V}, \quad \langle \mathbf{v} \rangle = \mathbf{V}, \quad \langle \mathbf{u} \rangle = 0, \quad (4)$$

where the angular brackets denote averaging. Theoretical considerations use ensemble averaging over the realizations of the turbulent flow. In processing the observational data, space or time averaging is employed. It is hoped that all averaging procedures give similar results.

Turbulence in stars results from convective instability. The convection regimes are strongly supercritical and non-linear (the Rayleigh numbers are much larger than the critical value), which leads to the development of turbulence. Such turbulent convection in stars has some particular features. As a rule, the velocities of turbulent motion are small compared to the speed of sound. Nevertheless, the compressibility of the medium cannot be neglected, because the motion occurs in a gravitational field, under conditions of substantial spatial inhomogeneities in density and other thermodynamic parameters (such a radial inhomogeneity is commonly termed *stratification*). The stratification in stellar convection zones is nearly adiabatic. This is because a well-developed convective instability, as most other instabilities, exhausts its own source. The source of convection is a superadiabatic stratification. Thus, although the stratification in convection zones is superadiabatic, it departs little from the adiabatic law. For example, the relative magnitude of this departure for the Sun is $\sim 10^{-4}$ [13]. For this reason, the turbulent flow gives rise to only minor fluctuations in the thermodynamic parameters, and the continuity equation can be written as

$$\operatorname{div}(\rho \mathbf{v}) = 0. \quad (5)$$

In contrast to the incompressible approximation, where $\operatorname{div} \mathbf{v} = 0$, Eqn (5) is termed the *inelastic approximation* [28, 29].

The averaged Eqn (3),

$$\frac{\partial \mathbf{V}}{\partial t} + (\mathbf{V} \cdot \nabla) \mathbf{V} + \frac{1}{\rho} \nabla P = \frac{1}{\rho} \nabla \cdot \mathbf{R}, \quad (6)$$

implies that the effect of turbulence on the mean, large-scale flow is described by the Reynolds stress tensor

$$R_{ij} = -\rho Q_{ij}, \quad Q_{ij} = \langle u_i u_j \rangle. \quad (7)$$

We have omitted the contribution of viscosity in Eqn (6) for the large-scale flow, because we assume large Reynolds numbers. The Reynolds stresses contain eddy viscosity, which is much larger.

It is convenient to use spherical coordinates (r, ϑ, ϕ) to describe large-scale flows in stars. We assume that the

rotational axis is the polar axis of the coordinate system. Let the large-scale flow and the averaged parameters of turbulence be axially symmetric. Then the mean flow includes a nonuniform rotation with an angular velocity $\Omega(r, \vartheta)$ and the so-called meridional circulation — a flow whose velocity vector \mathbf{V}^m lies in the meridional plane. As we see in what follows, a meridional circulation arises inevitably if the rotation is nonuniform. In view of condition (5), the meridional flow can be described by a stream function $\psi(r, \vartheta)$,

$$\mathbf{V} = \mathbf{e}_\phi r \sin \vartheta \Omega + \frac{1}{\rho} \operatorname{rot} \left(\mathbf{e}_\phi \frac{\psi}{r \sin \vartheta} \right), \quad (8)$$

where \mathbf{e}_ϕ is the azimuthal unit vector.

The azimuthal component of (6) yields an equation for the angular velocity,

$$\rho r^2 \sin^2 \vartheta \frac{\partial \Omega}{\partial t} = -\operatorname{div}(\rho r \sin \vartheta \langle u_\phi \mathbf{u} \rangle + \rho r^2 \sin^2 \vartheta \Omega \mathbf{V}^m). \quad (9)$$

The vector whose divergence is taken is the angular-momentum flux. A turbulent flow contributes to this flux provided that the nondiagonal components of correlation tensor (7), $Q_{\phi r}$ and $Q_{\phi \vartheta}$, do not vanish.

We assume that the rotation is uniform at some instant. If the turbulent flux of angular momentum differs from zero, the regions where the divergence of the flux is positive decelerate their rotation at later times and the regions where the divergence is negative accelerate their rotation. Thus, the rotation becomes nonuniform. The presence of nonzero turbulent fluxes of angular momentum in *uniformly* rotating media is called the *A-effect* [30]. To all appearances, this effect, discovered by Lebedinskii [26], is the basic source of differential rotation. If $\cos \vartheta Q_{\phi \vartheta}^A > 0$, the *A-effect* results in a relatively fast rotation of the equator, as is observed on the Sun. (We discuss the origin of the *A-effect* in Section 4.)

The emergence of effective transport coefficients, in particular, the eddy viscosity, seems to be the most widely known effect of turbulence on large-scale fields. Viscous, or dissipative, fluxes of angular momentum vanish in the case of a uniform rotation, but they are generally present in Reynolds stresses (7):

$$Q_{ij} = Q_{ij}^A + Q_{ij}^v. \quad (10)$$

Here, the first term on the right-hand side corresponds to the *A-effect* and the second to the contribution from the eddy viscosity.

In the first (fairly crude) approximation, the formation of differential rotation can be described as the establishment of a balance between the nondissipative angular-momentum fluxes and the effective viscosity. If the rotation is uniform, there are no dissipative fluxes of angular momentum, but the *A-effect* is present, and hence the corresponding nondissipative fluxes transfer angular momentum from the poles to the equator. A rotational nonuniformity then arises and grows with time. Dissipative fluxes from the equator to the poles, $\cos \vartheta Q_{\phi \vartheta}^v < 0$, also appear. The stronger the rotational nonuniformity, the larger they are. As a result, a steady differential rotation sets in, with the nondissipative and viscous fluxes of angular momentum balancing each other.

In such a steady state, the vector of the angular-momentum flux becomes solenoidal but not necessarily

zero. This is important to note in view of a long-standing fallacy related to fluxes of angular momentum. The concept of the A -effect suggested that the relatively fast rotation of the solar equator can be maintained provided that the correlation between the azimuthal and meridional motions has a definite sign, $\cos \vartheta Q_{\phi\vartheta} > 0$. Such a correlation was revealed for the motion of sunspots [31]. At a later time, however, the latitudinal dependence of the corresponding correlation (which came to be known as the ‘Ward profile’) was refined, and the quantity $Q_{\phi\vartheta}$ was found to be within observational errors [32, 33] or even to have a sign opposite to the expected one [34]. This was taken as a contradiction between theory and observations. However, in all likelihood, observations yield the full correlation (10), which includes contributions from both the A -effect and effective viscosities. Either sign of this quantity is compatible with the equatorial acceleration observed on the Sun (model calculations [35] yield $\cos \vartheta Q_{\phi\vartheta} < 0$ near the surface, in agreement with [34]). The story of the Ward profile is in no way a unique example of a situation in which an almost obvious statement proves to be wrong.

3.2 Meridional circulation

We now turn to the second term on the right-hand side of Eqn (9). It takes the contribution of the meridional circulation to the angular-momentum flux into account. This contribution is not responsible for the onset of differential rotation, but it proves to be highly important. The meridional circulation cannot be neglected. As Kippenhahn [36] showed for the first time, the meridional circulation emerges inevitably if a differential rotation is present. This fact imposes substantial limitations on the well-established distributions of angular velocity in stars.

The A -effect does not directly influence the meridional circulation, which is only weakened by turbulence via the eddy viscosity. The dissipative component of the correlation of fluctuating velocities (10) is determined by the tensor of eddy viscosities \mathcal{N} :

$$Q_{ij}^v = -\mathcal{N}_{ijkl} \frac{\partial V_k}{\partial r_l}. \quad (11)$$

In the simplest case of isotropic turbulence, only two transport coefficients are present:

$$\mathcal{N}_{ijkl} = \nu_T \left(\delta_{ik} \delta_{jl} + \delta_{il} \delta_{jk} - \frac{2}{3} \delta_{ij} \delta_{kl} \right) + \mu_T \delta_{ij} \delta_{kl}. \quad (12)$$

Rotating turbulence normally exhibits a substantial anisotropy, and hence the eddy viscosities have a more complex form (34).

The equation for the meridional circulation, which we assume to be stationary, can be obtained as the azimuthal component of the curl of Eqn (6) for the mean velocity [25, 37],

$$\mathcal{D}(\psi) = \sin \vartheta r \frac{\partial \Omega^2}{\partial z} - \frac{g}{c_p r} \frac{\partial S}{\partial \vartheta}, \quad (13)$$

where we omit the small, second-order contribution with respect to the velocity of the meridional flow; $z = r \cos \vartheta$ is the spatial coordinate measured along the rotational axis (the distance from the equatorial plane); g is the gravity acceleration; $S = c_v \ln(P/\rho^\gamma)$ is the specific entropy of the ideal gas;

and c_p and c_v are the specific heats at constant pressure and volume, respectively.

The left-hand side of Eqn (13) takes the contribution of turbulent viscosities into account,

$$\mathcal{D}(\psi) = -(\mathbf{e}_\phi)_n \varepsilon_{nmi} \frac{\partial}{\partial r_m} \left(\frac{1}{\rho} \frac{\partial}{\partial r_j} \rho \mathcal{N}_{ijkl} \frac{\partial V_k^m}{\partial r_l} \right). \quad (14)$$

The explicit form of this contribution is extremely unwieldy, but it is not needed in the subsequent discussion. It is only important to remember that the left-hand side of Eqn (13) includes the viscous drag to the meridional flow. Two sources of meridional circulation are written on the right-hand side.

The first source is the conservative part of the centrifugal force. This force can be expressed in terms of the centrifugal potential only if the angular velocity is constant at rotationally coaxial cylindrical surfaces, i.e., is independent of the z coordinate. If so, the centrifugal force can be balanced by the pressure and has no effect. However, the sources of differential rotation produce a z -dependent distribution of angular velocity. In this case, the centrifugal force gives rise to a meridional circulation. If, for example, the angular velocity increases along the z axis toward the equatorial plane, the arising centrifugal-force moment results in a meridional circulation that is directed from the equator to the poles at the surface of the star and is closed through an equatorward flow deep in the convection zone. It can be verified that these qualitative considerations agree with the sign of the first term on the right-hand side of Eqn (13). The characteristic value of the ratio of this contribution to the left-hand side of Eqn (13) is the Taylor number

$$\text{Ta} = \frac{4\Omega^2 R^4}{v_T^2}. \quad (15)$$

This quantity is large for the Sun, $\text{Ta} \simeq 10^7$. Therefore, the centrifugal force cannot be balanced by the viscous drag counteracting the meridional flow. If we neglect the baroclinic contribution in the equation for the meridional flow (the second term on the right-hand side), the meridional flow stabilizes as its source is exhausted: the meridional circulation produces an angular-momentum flux [see Eqn (9)] that changes the nonuniform rotation such that the angular velocity becomes virtually constant on cylindrical surfaces. Such a mode of rotation can be considered a particular implication of the Taylor–Proudman theorem [38].

For this reason, some numerical models of the differential rotation of the Sun yielded cylindrical isorotational surfaces [39–42]. This rotational state seemed to necessarily set in at high Taylor numbers. However, it contradicts helioseismological data. For a long time, this contradiction was among the most serious difficulties of the theory of differential rotation and even received the proper name ‘the Taylor number puzzle’ [43].

It can, however, be resolved based on Eqn (13) by taking the baroclinic source of meridional circulation into account [37, 44–46] — the second term on the right-hand side of Eqn (13). This contribution is called baroclinic because it results from the discrepancy between the isobaric and constant-density surfaces (see, e.g., Ref. [25]):

$$\rho^{-2} (\nabla P \times \nabla \rho)_\phi = \frac{g}{c_p r} \frac{\partial S}{\partial \vartheta}.$$

For the Sun, the ratio of this contribution to the left-hand side of the equation is typically of the same order of magnitude as the Taylor number.

Equation (13) for the meridional circulation proves to be highly informative. In particular, it indicates that the distribution of angular velocity in the convection zone is determined by the balance between the centrifugal and baroclinic sources of meridional flow (the Taylor–Proudman balance). As we see in what follows, Eqn (13) can be used to estimate the expected magnitude of the differential rotation and even predict the character of its dependence on the mass of the star. Two other points important for the theory of differential rotation are also related to the meridional circulation.

The speed of the meridional circulation is controlled by the small disbalance between the centrifugal and baroclinic sources. Therefore, the inverse problem of determining the meridional flow from the given distributions of angular velocity and temperature is ill-posed. Small variations in these distributions result in large variations in the meridional flow. For this reason, attempts at inferring the meridional circulation from the observed temperature and angular-velocity distributions can hardly be successful [47].

The balance between the two sources of differential rotation holds for the bulk of the convective envelope of the star but is violated near its boundaries. This is because the Taylor–Proudman balance contradicts the boundary conditions, and boundary layers of thickness $d \sim R Ta^{-1/4}$ are formed near the surfaces of the convection zone at high Taylor numbers (15). Such layers are well known as Ekman layers [38] in geophysics, which deals with characteristic Taylor numbers even larger than for the Sun (the Ekman number is $E = 2/Ta^{1/2}$). Likely, the violation of the Taylor–Proudman balance near the boundaries revealed in numerical simulations of solar convection [48] is related precisely to these layers. The boundary layers impose more stringent requirements on the spatial resolution of numerical simulations.

Observations detect meridional circulation on the Sun. Direct Doppler measurements reveal a flow at the solar surface, from the equator to the poles, with the amplitude $\sim 10 \text{ m s}^{-1}$ [49]. Recently, helioseismological indications for the meridional flow were found [50]. The flow directed to the poles is present at depths up to 12 Mm (no data are available for deeper layers). This flow is dominant. Against its background, a time-dependent flow of a smaller amplitude is defined, which converges to the latitude where the frequency of sunspot formation is at a maximum. This latitude of highest sunspot activity varies with time, and the convergent meridional flow varies accordingly [50].

As we have ascertained, the helioseismological data on the internal rotation of the Sun could hopefully be understood only with due account for the baroclinic source of meridional circulation — the second contribution on the right-hand side of Eqn (13). Otherwise, the rotation inevitably features cylindrical isorotational surfaces, in contradiction to the available data. To consider the baroclinic circulation, we must find why the temperature can depend on the latitude in stellar convection envelopes. This issue can be resolved by considering heat transfer in rotating turbulent media.

3.3 Convective heat transport

To describe the baroclinic source of meridional circulation contained in Eq (13), it is convenient to use the equation for

the specific entropy (see, e.g., Ref. [51])

$$\rho T \left(\frac{\partial S}{\partial t} + (\mathbf{V}^m \cdot \nabla) S \right) = -\text{div}(\mathbf{F}^{\text{conv}} + \mathbf{F}^{\text{rad}}) + \epsilon. \quad (16)$$

Here, \mathbf{F}^{rad} is the heat flux due to the diffusion of photons (for solar-type stars, the molecular heat conduction can, as a rule, be neglected), \mathbf{F}^{conv} is the convective heat flux, and ϵ is the source function.

The heat flux

$$F_i^{\text{conv}} = -\rho T \chi_{ij} \frac{\partial S}{\partial r_j} \quad (17)$$

is controlled by the effective thermal diffusivity tensor χ_{ij} . Thermal diffusion is not isotropic, because certain directions are distinguished by the rotation and stratification. The stratification, however, has no substantial effects, because the corresponding distinguished (radial) direction does not violate the spherical symmetry in the distribution of the thermodynamic parameters of the fluid. Deviations from the spherical symmetry are associated with rotation:

$$\chi_{ij} = \chi_T \left(\phi(\Omega^*) \delta_{ij} + \phi_{\parallel}(\Omega^*) \frac{\Omega_i \Omega_j}{\Omega^2} \right). \quad (18)$$

Here, χ_T is the isotropic turbulent thermal diffusivity for a nonrotating fluid, the functions ϕ and ϕ_{\parallel} (see Section 4.4, Fig. 9) take the effects of rotation into account, and Ω^* is the angular velocity (25) made dimensionless in an appropriate way. For a nonrotating fluid, $\phi(0) = 1$, $\phi_{\parallel}(0) = 0$, and the thermal diffusivity becomes isotropic. Formula (18) accounts for the fact that turbulence, when affected by rotation, becomes anisotropic and approaches a two-dimensional state [52], with the correlation length and the rms velocity in the direction of the rotational axis exceeding the corresponding quantities for transverse directions. Therefore, the effective thermal diffusivity along the rotational axis, χ_{\parallel} , exceeds the transversal diffusivity by $\chi_{\parallel} - \chi_{\perp} = \chi_T \phi_{\parallel}$. Rotation has two important implications.

First, the transport coefficient for the radial direction depends on the latitude,

$$\chi_{rr} = \chi_T (\phi(\Omega^*) + \phi_{\parallel}(\Omega^*) \cos^2 \vartheta). \quad (19)$$

Second, the nondiagonal components of the thermal-diffusivity tensor differ from zero,

$$\chi_{r\vartheta} = \chi_{\vartheta r} = -\chi_T \phi_{\parallel}(\Omega^*) \cos \vartheta \sin \vartheta. \quad (20)$$

As a result, the temperature becomes latitude-dependent. Nondiagonal components (20) are especially important in this case, because they produce meridional heat fluxes due to the (dominant) radial nonuniformity of specific entropy. The inclusion of the latitudinal dependence of thermal diffusivity (19) alone does not resolve the Taylor number puzzle [43].

The influence of rotation on the convective heat transport renders the polar regions of the star slightly hotter than the equatorial zone. The resulting buoyancy force acts so as to produce a meridional flow from the poles to the equator near the surface of the star and from the equator to the poles in deep layers: the relatively hot fluid spreads over the surface from the poles, while the relatively cool substance sinks at the equator. Therefore, the baroclinic source of meridional flow

in Eqn (13) counteracts the centrifugal source, which results in a deflection of isorotational surfaces from cylinders and ultimately brings the calculated differential rotation into agreement with helioseismological data.

The baroclinic and centrifugal sources of meridional circulation are of the same order of magnitude if $\Delta T/T \sim R\Delta\Omega\Omega/g \sim 10^{-5}$ (we take $R_\odot = 6.9 \times 10^{10}$ cm and the surface gravity acceleration $g = 2.7 \times 10^4$ cm s $^{-2}$). The characteristic temperature in the convective envelope comprises several hundred thousand degrees. To resolve the Taylor number puzzle, the ‘differential temperature’ $T' \sim 1$ K is required. Such a temperature variation seems to be tiny and insignificant for the huge and hot Sun; however, if present permanently, it has substantial effects on the global circulation of the solar material. Moreover, convective motions can only influence the distribution of the so-called potential temperature ΔT , i.e., the radially integrated superadiabatic gradient $\nabla\Delta T = \nabla T - \mathbf{g}/c_p$. The characteristic potential temperature is $\Delta T \sim 10$ K. Therefore, the needed differential temperature is of the order of 10% of the maximum possible value, thus being not so small.

Some attempts have been made to detect the differential temperature on the Sun. They were largely stimulated by the theory of differential rotation. No success has been achieved. Only an upper bound of about 5 K was found for T' [53, 54]. There is indication that the actual differential temperature on the Sun is indeed about 1 K [55].

The source function in Eqn (16) is related to Reynolds stress tensor (7) [51],

$$\epsilon = R_{ij} \frac{\partial V_i}{\partial r_j} = -\rho(Q_{ij}^A + Q_{ij}^v) \frac{\partial V_i}{\partial r_j}, \quad (21)$$

where Eqn (10) is taken into account. In mean-field fluid mechanics, the energy exchange between the mean flow and turbulent medium is determined not only by the eddy viscosity but also by the A -effect [56]. The latter is frequently overlooked, which results in contradictions. For the solar convection zone, the heating power due to eddy viscosity taken alone would be comparable to the luminosity of the Sun [57]. In reality, such heating is obviously impossible. The situation can be amended by taking the nondissipative stresses (A -effect) into account. In view of boundary condition (45), source function (21) vanishes when integrated over the volume of the convection zone, as dictated by the energy conservation condition. This source is usually neglected in calculations of the differential rotation.

4. Mean-field effects of turbulence

We found out in Section 3 *which* effects involved in the problem of differential rotation are produced by turbulence. Our aim at this stage is to understand *how* this occurs. It can also be said that we have considered the flows whose characteristic spatial scale is much larger than the correlation scale of turbulent flows, ℓ . In this section, we pay principal attention to flows of scale ℓ and shorter.

To describe the differential rotation, we have to determine the nondissipative fluxes of angular momentum produced by turbulence and the effective transport coefficients — eddy viscosity and eddy thermal diffusivity. Strictly speaking, this does not necessarily imply the calculation of the characteristics of turbulence. The unknown quantities may be free

parameters of the models. Such assumptions were formerly normal, but all models of this sort were at variance with observations. This can easily be understood: there were too many free parameters. Wandering in the parameter space at random can scarcely lead one into the ‘needed’ region. Usually, the number of free parameters is reduced by setting some of them to zero, but in no way did this reduce the arbitrariness of the ‘parametric’ models. A breakthrough came when all the turbulent parameters needed to model the differential rotation were computed based on a unified approach, possibly crude but common to all calculations.

The physics of small-scale phenomena may evidently also be of interest irrespective of the simulation of large-scale flows.

4.1 Quasilinear approximation

The basic problem stems from the fact that no reliable methods for treatment of turbulence are available. The phenomenon of turbulence is extremely difficult to describe because of its nonlinear and nonequilibrium nature [27, 58]. However, mean-field fluid mechanics requires describing the effects of turbulence on the averaged fields rather than dealing with turbulence itself. To a certain extent, this improves the situation. The resulting problems can be tackled using the well-reputed, although not strictly substantiated, quasilinear approximation (in the mean-field theory, it is also known as *first-order smoothing* [59] or the *second-order correlation approximation* [52]).

This approximation enables one to find Reynolds stresses (7) from the equation for the fluctuating velocity, which can be obtained by subtracting mean-velocity equation (6) from the original equation of motion (3),

$$\begin{aligned} \frac{\partial \rho u_i}{\partial t} - \frac{\partial \sigma_{ij}(\mathbf{u})}{\partial r_j} + \frac{\partial}{\partial r_j} (\rho u_i u_j - \rho \langle u_i u_j \rangle) \\ = 2\rho e_{ijk} u_j \Omega_k - \frac{1}{\rho} \frac{\partial P'}{\partial r_i} - \frac{\partial}{\partial r_j} (\rho u_i V_j + \rho u_j V_i), \end{aligned} \quad (22)$$

where P' is the fluctuating pressure. The equation is written here in a rotating frame of reference, and the Coriolis force is present on its right-hand side. The nonlinear terms on the left-hand side prevent us from solving this equation. For this reason, it is the practice to either drop the nonlinear terms or to replace the entire left-hand side of Eqn (22) with a τ -relaxing term,

$$\frac{\partial \rho u_i}{\partial t} - \frac{\partial \sigma_{ij}(\mathbf{u})}{\partial r_j} + \frac{\partial}{\partial r_j} (\rho u_i u_j - \rho \langle u_i u_j \rangle) = \rho \frac{u_i}{\tau}, \quad (23)$$

where $\tau = \ell/\langle u^2 \rangle^{1/2}$ is the characteristic time of nonlinear interactions and ℓ is the characteristic scale of turbulent motions. Various terms are used to denote the approximation in (23). We call it the *mixing-length approximation*, following Durney and Spruit [60], who first applied it to the problem of differential rotation. The quasilinear approximation consists precisely in neglecting the nonlinear terms in Eqn (22). It can be justified in the case of short correlation times τ_{corr} of fluctuating velocities, $\tau_{\text{corr}} \ll \tau$. For a short-time-correlated random flow, the quasilinear approximation is rigorous and cannot yield results forbidden by any physical laws. In reality, however, $\tau_{\text{corr}} \simeq \tau$. It is a widespread opinion that the mixing-length approximation, fairly crude as it is, more closely corresponds to real conditions than the quasilinear approximation does. Formally, however, the quasi-

linear approximation is in no respect worse, offering a more general approach: the mixing-length approximation can be obtained from the quasilinear approximation as a limiting case [61], while no inverse limiting process seems to exist.

All the parameters of turbulence needed for the theory of differential rotation have been calculated in the quasilinear approximation (the results can be found in the literature cited below). Nevertheless, the quantitative models of differential rotation are based on the mixing-length approximation. The point is that the quasilinear expressions — e.g., for the eddy viscosity — contain spectral functions of turbulence unknown for the solar turbulent convection. For this reason, the corresponding formulas of the mixing-length theory are used. They contain only well-known quantities and lead to mathematical simplifications. Our further presentation is based solely on the mixing-length approximation.

Virtually all calculations for the problems under discussion reduce to the evaluation of the effects of rotation on turbulence. In fact, two kinds of turbulence are considered. The first one, which is usually called the *original* turbulence, would be present in a nonrotating medium, given the actual sources of turbulence. The original turbulence is normally assumed to be given. The parameters of the turbulence in the rotating medium are calculated from the properties of the original turbulence.

For mathematical convenience, we use the (solenoidal) momentum density $\mathbf{m} = \rho \mathbf{u}$ (5) instead of the velocity of the (compressible) flow and we apply the Fourier transform with respect to the spatial coordinates,

$$\mathbf{m}(\mathbf{r}) = \int \exp(i\mathbf{k} \cdot \mathbf{r}) \hat{\mathbf{m}}(\mathbf{k}) d\mathbf{k}.$$

This reduces the partial differential equations to algebraic equations for the Fourier amplitudes, and hence the following linear relation between the momentum densities for the original and rotating turbulence can be obtained [62, 63]:

$$\hat{m}_i(\mathbf{k}) = D_{ij}(\boldsymbol{\Omega}, \mathbf{k}) \hat{m}_j^\circ(\mathbf{k}), \quad D_{ij}(\boldsymbol{\Omega}, \mathbf{k}) = \frac{\delta_{ij} + \Omega^* \mu \varepsilon_{ijn} k_n / k}{1 + \Omega^{*2} \mu^2}, \quad (24)$$

where the superscript $^\circ$ refers to the original turbulence, $\mu = \cos(\boldsymbol{\Omega}\mathbf{k})$ is the cosine of the angle between the wavevector and angular velocity, and the Coriolis number

$$\Omega^* = 2\tau\Omega \quad (25)$$

characterizes the intensity of interaction between the turbulent convection and rotation.

Equation (24) can be used to express the parameters of the rotating turbulence in terms of the Coriolis number and the parameters of the original turbulence. We recall, however, that the hypothetical original turbulence does not actually exist, but it would occur in a nonrotating medium in the presence of the actual sources of turbulence (actual superadiabatic gradient). Therefore, its intensity can be found from the relation for a nonrotating medium (see, e.g., Refs [13, 64]),

$$\langle u^2 \rangle^\circ = -\frac{\ell^2 g}{4c_p} \frac{\partial S}{\partial r}, \quad (26)$$

where the entropy S must be determined from heat transfer equation (16).

4.2 The Λ -effect

As mentioned in Section 3, the Λ -effect is defined as the presence of turbulent fluxes of angular momentum under conditions of a uniform rotation [30, 52]. The uniformity of rotation is noted to emphasize that these fluxes are not related to dissipation, i.e., to the action of eddy viscosity.

We begin discussing the Λ -effect with a qualitative consideration of the factors that give rise to this effect. Figure 5 schematizes motions in a rotating medium. The dashed arrows show the original motions and the solid arrows show the motions perturbed by the Coriolis force. It can easily be understood that convective mixing in the radial direction transfers angular momentum into the depths of the convection zone (the left-hand part of the figure). If the direction of the original motion is radial ($u_r^\circ > 0$), the Coriolis force deflects the moving fluid parcel counter to the global rotation with the characteristic velocity

$$u_\phi \simeq -2\tau\Omega u_r^\circ \sin \vartheta.$$

The product of the radial and azimuthal velocities is negative:

$$u_r u_\phi \simeq -\Omega^* u_r^{\circ 2} \sin \vartheta < 0.$$

If the original motion is directed against the radius ($u_r < 0$), the fluid parcel deflects in the direction of the global rotation. For the product $u_r u_\phi$, we obtain the same estimate, and averaging over ascending and descending original motions yields a negative radial flux of angular momentum:

$$\langle u_r u_\phi \rangle \simeq -\Omega^* \langle u_r^2 \rangle^\circ \sin \vartheta < 0.$$

It is important that the azimuthal original motions give the opposite effect (see the right-hand part of Fig. 5). In this case, similar considerations lead to the estimate

$$\langle u_r u_\phi \rangle \simeq \Omega^* \langle u_\phi^2 \rangle^\circ \sin \vartheta > 0.$$

Horizontal mixing carries angular momentum to the surface of the convection zone. Adding the contributions of radial and azimuthal motions yields

$$Q_{r\phi}^\Lambda \simeq \Omega^* (\langle u_\phi^2 \rangle^\circ - \langle u_r^2 \rangle^\circ) \sin \vartheta \quad (27)$$

for the radial Λ -effect.

This equation demonstrates the following important fact: for the onset of differential rotation, the original turbulence must be anisotropic. This was first noted by Lebedinskii [26] and then, independently, by Wasiutynski [65]. A radial angular-momentum flux arises provided that the character-

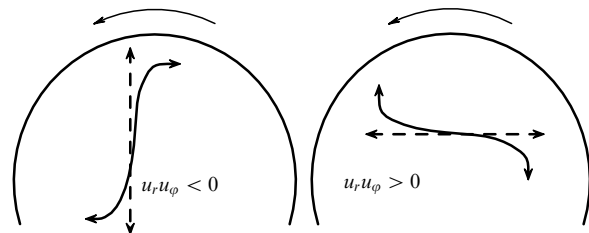


Figure 5. The origin of angular-momentum fluxes due to the effect of the Coriolis force on the original turbulence. Dashed arrows show original motions; solid arrows show motions disturbed by rotation.

istic velocities of radial and azimuthal motions in the original turbulence are different.

Estimates similar to the above-presented ones can be used to ascertain that the origin of a meridional angular-momentum flux requires the presence of a distinguished direction in the horizontal plane, i.e., a difference between azimuthal and meridional motions. This entails some difficulty, because there are no factors that could produce a horizontal anisotropy in a nonrotating original turbulence. Nevertheless, a meridional flux of angular momentum is needed, because precisely a latitudinal rotational non-uniformity is observed on the Sun.

This difficulty can be overcome in different ways. The following one proves to be most effective. Our estimates, including formula (27), are valid for slow rotation, i.e., for small Coriolis numbers (25), $\Omega^* \ll 1$. The Coriolis force transforms radial velocities into azimuthal velocities (see Fig. 5). Therefore, in a rotating medium, the counterpart of a radially anisotropic original turbulence has the form of an anisotropic turbulence in which a horizontal anisotropy is also present. Such anisotropy is to appear in the second order with respect to the Coriolis number, while the emergence of a meridional A -effect in the next (third) order can be expected if the original turbulence is only radially anisotropic. Calculations of contributions up to the third order in the Coriolis number confirmed these expectations [66, 67].

The Coriolis number on the Sun depends on the radius r . It is smaller than unity near the surface but exceeds 10 at the base of the convection zone, with the mean value $\Omega^* \simeq 6$ (see Section 5.3.1, Fig. 13). States with $\Omega^* > 1$ are typical of solar-type stars [68]. This means that the inclusion of contributions nonlinear in Ω^* is justified but entails a new difficulty. There is no reason to restrict the consideration to contributions of up to the third order in the Coriolis number. Contributions of all orders should be taken into account. A theory suited to stellar conditions should be fully nonlinear in Ω^* [69].

If only the radial direction is distinguished in original turbulence, the nondissipative part of correlation tensor (10) can only have the following structure:

$$Q_{ij}^A = v_T \Omega_k n_l \left(U(\Omega^*) (n_i \varepsilon_{jkl} + n_j \varepsilon_{ikl}) - H(\Omega^*) \frac{(\mathbf{n} \cdot \boldsymbol{\Omega})}{\Omega^2} (\Omega_i \varepsilon_{jkl} + \Omega_j \varepsilon_{ikl}) \right). \quad (28)$$

Here, v_T is the isotropic eddy viscosity (see Section 4.3), \mathbf{n} is the unit vector directed radially, and U and H are the dimensionless functions that determine the fluxes of angular momentum in the radial direction and along the rotational axis, respectively:

$$\begin{aligned} Q_{\phi r}^A &= v_T \Omega \sin \vartheta (U - H \cos^2 \vartheta), \\ Q_{\phi \vartheta}^A &= v_T \Omega H \cos \vartheta \sin^2 \vartheta. \end{aligned} \quad (29)$$

Calculations of the A -effect for an anisotropic original turbulence without considering the inhomogeneity of the medium yield [62, 63]

$$U(\Omega^*) = 2aI_0(\Omega^*), \quad H(\Omega^*) = 2aI_1(\Omega^*), \quad (30)$$

where a is the anisotropy parameter,

$$a = \frac{\langle u_r^2 \rangle^\circ}{\langle u_\vartheta^2 \rangle^\circ} - 1, \quad -1 < a < 1. \quad (31)$$

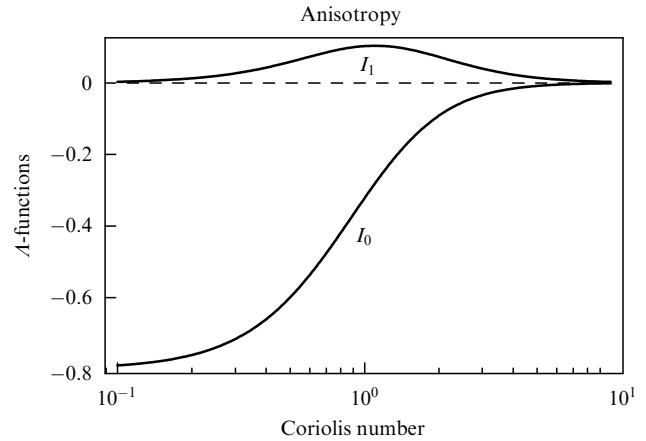


Figure 6. The dimensionless fluxes of angular momentum (29)–(31) as functions of the Coriolis number. At large values of the argument, both components are proportional to Ω^{*-3} .

The upper bound on the anisotropy parameter holds because the spectral functions of the velocity fluctuations are positive [27]. The functions I_1 and I_0 are shown in Fig. 6.

For small Coriolis numbers ($\Omega^* \ll 1$),

$$U = -\frac{4a}{5}, \quad H = O(\Omega^{*2}).$$

This means that the meridional angular-momentum flux is small, while the radial flux is directed downward (is negative) if the mixing is mainly radial and is directed to the surface if horizontal velocities dominate, in accordance with above qualitative considerations.

In the opposite limiting case of fast rotation ($\Omega^* \gg 1$), function (30) is inversely proportional to the third power of the Coriolis number:

$$U = -\frac{H}{3} = -\frac{3a\pi}{8\Omega^{*3}}.$$

This result may seem strange, because U and H cannot depend on the direction of rotation, i.e., they must be even functions of the angular velocity. This is actually the case, as can be seen, for example, from the explicit form of the function $I_1(\Omega^*)$ given by the first formula in (30):

$$I_1(\Omega^*) = \frac{3}{4\Omega^{*4}} \left(-15 + \frac{2\Omega^{*2}}{1 + \Omega^{*2}} + \frac{3\Omega^{*2} + 15}{\Omega^*} \arctg(\Omega^*) \right). \quad (32)$$

Function (32) is even but proportional to Ω^{*-3} at large Ω^* values.

A finding of exceptional importance for the theory of differential rotation was the establishment of the fact that not only anisotropy but also the nonuniformity of the turbulent medium gives rise to the A -effect. The density inhomogeneity is most significant [70, 71]. The density stratification with inelasticity condition (5) taken into account affects the turbulence. Anisotropy arises inevitably in this case [72], but the resulting A -effect cannot be attributed to this anisotropy taken alone.

The nondissipative fluxes of angular momentum that result from the density inhomogeneity of the turbulent

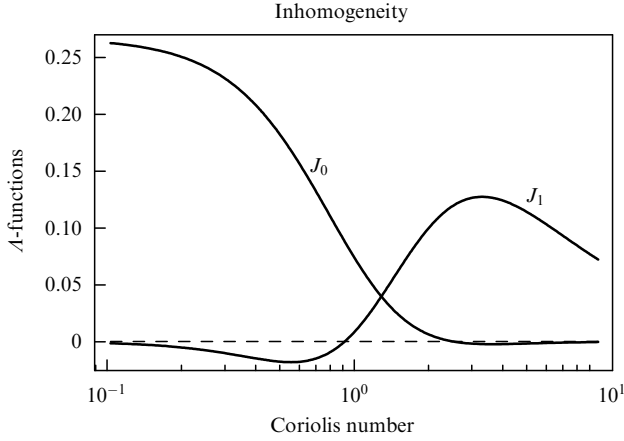


Figure 7. Angular-momentum fluxes (33) that result from density inhomogeneity, as functions of Coriolis number (25). At large Coriolis numbers, $J_1 \sim 1/\Omega^*$.

medium are still given by formula (29); in this case, however,

$$U = \left(\frac{\ell}{H_\rho} \right)^2 J_0(\Omega^*), \quad H = \left(\frac{\ell}{H_\rho} \right)^2 J_1(\Omega^*), \quad (33)$$

where $H_\rho = -1/(d \ln(\rho)/dr)$ is the density inhomogeneity scale and the functions J_0 and J_1 are plotted in Fig. 7.

We note once again that in the limiting case of slow rotation, only the radial flux of angular momentum is nonvanishing: $J_0(0) = 4/15$ and $J_1(0) = 0$ [71]. In the opposite limiting case where $\Omega^* \gg 1$, which is more important for applications, we have $J_1 = \pi/(4\Omega^*)$ and $J_0 = O(\Omega^{*-3})$. The fact that the Λ -effect under conditions of fast rotation is inversely proportional to the Coriolis number does not imply that the rotation is weakly differential [35], because the effective viscosities, as we see below, behave similarly. It is very important that at large Coriolis numbers, the contribution of the inhomogeneity to the Λ -effect exceeds the contribution of the anisotropy. This fact is not yet completely understood. Possibly, the reason is that a fast rotation can substantially affect the anisotropy of turbulence but has virtually no influence on the stratification. A comparison between Figs 6 and 7 shows that even for the Sun, at $\Omega^* \simeq 6$, the inhomogeneity makes the principal contribution; this contribution is absolutely dominant for young stars with rotational periods of several days.

This proves to be very advantageous to the theory. The fact is that the anisotropy of stellar convection has not yet been adequately studied. If it were significant, this would provide a free parameter to the models of differential rotation. However, the anisotropy plays no role in the case where $\Omega^* \gg 1$, which is typical for the overwhelming majority of stars. Only the inhomogeneity, which is known to a high accuracy for stellar convective envelopes, is important. As noted in Section 3.1, the stratification in the convection zones differs little from the adiabatic stratification. It is for this reason that, in essence, the contemporary models of differential rotation contain no free parameters.

4.3 Effective viscosities

Effective viscosities (11) are given by expression (12) only in the simplest case of isotropic turbulence and a nonrotating fluid. Rotation results in anisotropy and the tensor of effective viscosities becomes considerably more complicated.

In this section, we disregard the anisotropy of the original turbulence and the effects of the nonuniformity of the medium, considered when calculating the λ effect. The perturbation technique allows such an approximation: the nonuniform flow in (11) results from either anisotropy or inhomogeneity, which have already been taken into account in the Λ -effect. The large-scale velocity \mathbf{V} in (11) already implicitly contains the contribution of the anisotropy of turbulence and/or the inhomogeneity. There is no need to take these contributions into account once again, in calculating \mathcal{N} . We revisit this circumstance somewhat later.

The effective viscosities for a rotating medium were calculated in Ref. [73]:

$$\begin{aligned} \mathcal{N}_{ijkl} = & v_1(\delta_{ik}\delta_{jl} + \delta_{jk}\delta_{il}) + v_2 \left(\delta_{il} \frac{\Omega_j \Omega_k}{\Omega^2} + \delta_{jl} \frac{\Omega_i \Omega_k}{\Omega^2} \right. \\ & + \delta_{ik} \frac{\Omega_j \Omega_l}{\Omega^2} + \delta_{jk} \frac{\Omega_i \Omega_l}{\Omega^2} + \delta_{kl} \frac{\Omega_i \Omega_j}{\Omega^2} \Big) \\ & + v_3 \delta_{ij} \delta_{kl} - v_4 \delta_{ij} \frac{\Omega_k \Omega_l}{\Omega^2} + v_5 \frac{\Omega_i \Omega_j \Omega_k \Omega_l}{\Omega^4}. \end{aligned} \quad (34)$$

The coefficients in this equation depend on the Coriolis number (25),

$$v_n = v_T \phi_n(\Omega^*), \quad v_T = \frac{4}{15} \tau \langle u^2 \rangle^\circ, \quad (35)$$

where v_T is the effective viscosity for a nonrotating medium, which can be expressed in terms of the deviation from the adiabatic stratification according to formula (26). Explicit forms of the functions $\phi_n(\Omega^*)$ are given in Ref. [73]. Their Ω^* -dependences are shown in Fig. 8. For a rotating medium, only v_1 and v_3 differ from zero, and Eqn (34) changes into Eqn (12). In the case of fast rotation, all effective viscosities are inversely proportional to the Coriolis number: $\phi_n = O(\Omega^{*-1})$.

The complex structure of tensor (34) indicates that the effective viscosity depends on the relative orientation of the velocity vector and the direction in which the velocity is not uniform, as well as on the position of these directions with respect to the rotational axis. For example, in the case of a shear flow in which both the velocity and its gradient are normal to the rotational axis, the viscosity $v_{\perp\perp} = v_1$ is in

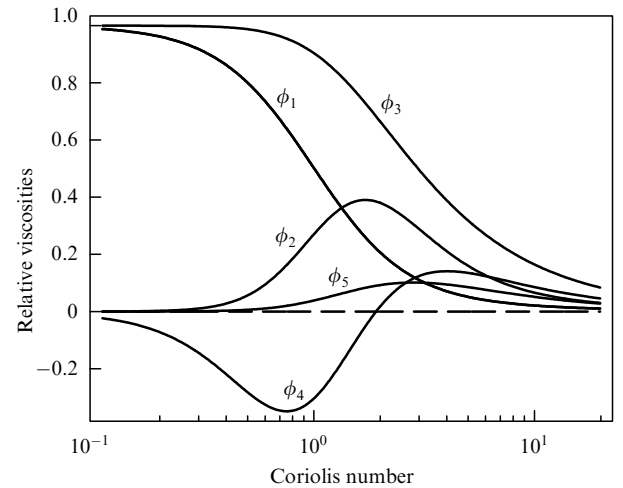


Figure 8. Relative viscosities ϕ_n that enter Eqn (35) as functions of Ω^* . At large argument values, all viscosities are proportional to Ω^{*-1} .

effect. The viscosity $v_{\perp\parallel} = v_1 + v_2$ applies to the normal velocity with an axially directed gradient. The equal viscosity $v_{\parallel\perp} = v_{\perp\parallel}$ acts if the velocity of the shear flow is parallel to the rotational axis, nonuniform in the direction normal to this axis, etc. Finally, we write the viscous fluxes of angular momentum that counteract the nondissipative fluxes (29) [62, 44]:

$$\begin{aligned} Q_{\phi r}^v &= -v_1 r \sin \vartheta \frac{\partial \Omega}{\partial r} - v_2 \sin \vartheta \cos \vartheta \left(r \cos \vartheta \frac{\partial \Omega}{\partial r} - \sin \vartheta \frac{\partial \Omega}{\partial \vartheta} \right), \\ Q_{\phi \vartheta}^v &= -v_1 \sin \vartheta \frac{\partial \Omega}{\partial \vartheta} - v_2 \sin^2 \vartheta \left(\sin \vartheta \frac{\partial \Omega}{\partial \vartheta} - r \cos \vartheta \frac{\partial \Omega}{\partial r} \right). \end{aligned} \quad (36)$$

Two other points related to the effective viscosities should be mentioned.

In relatively old studies [26, 65, 66, 74], anisotropic viscosity rather than nondissipative fluxes of angular momentum (the Λ -effect, see Section 4.2) was regarded as the reason for differential rotation. Above, we considered the fluxes of angular momentum in a rotating frame of reference and determined the full nonlinear dependences of their nondissipative and viscous components on the rotational velocity of the medium, which was in fact the angular velocity of the frame of reference. In principle, another, more compact procedure of determining the same parameters is possible. For an inertial frame of reference, only the second term Q^v , Eqn (11), can be present in correlation tensor (10), while Q^A must be zero. This follows from the Galilean invariance of Reynolds stresses (7).

This does not contradict the above discussion. The fact is that anisotropic turbulence leads to a tensor of effective viscosities that does not satisfy the symmetry principle for the kinetic coefficients, $\mathcal{N}_{ijkl} = \mathcal{N}_{klij}$ [75] (definition (7) only implies symmetry with respect to the permutation of the first two indices, $\mathcal{N}_{ijkl} = \mathcal{N}_{jikl}$). For a uniform rotation $\mathbf{V} = \mathbf{e}_\phi r \sin \vartheta \Omega$, we find from formula (11) that

$$\begin{aligned} Q_{\phi r} &= (\mathcal{N}_{r\phi r\phi} - \mathcal{N}_{r\phi\phi r}) \sin \vartheta \Omega + (\mathcal{N}_{r\phi\vartheta\phi} - \mathcal{N}_{r\phi\phi\vartheta}) \cos \vartheta \Omega, \\ Q_{\phi \vartheta} &= (\mathcal{N}_{\vartheta\phi r\phi} - \mathcal{N}_{\vartheta\phi\phi r}) \sin \vartheta \Omega + (\mathcal{N}_{\vartheta\phi\vartheta\phi} - \mathcal{N}_{\vartheta\phi\phi\vartheta}) \cos \vartheta \Omega. \end{aligned} \quad (37)$$

These expressions correspond to nondissipative fluxes of angular momentum, i.e., to the Λ -effect. In other words, the Reynolds stresses used in the theory of differential rotation can in principle be described in terms of the tensor of eddy viscosities only. For this, the viscosity tensor should be calculated with the anisotropy of turbulence and the full dependence of this tensor on the mean velocity taken into account. However, such a program can hardly be implemented in practice. Much more progress can be achieved if the calculations are carried out for a rotating frame of reference, with the nondissipative and dissipative components of the stress tensor separated. In addition, such a ‘unified approach’ results in confusion due to the introduction of the large-scale-flow generation effects involving the quantities formally called viscosities. We note that tensor (34) satisfies the symmetry principle for the kinetic coefficients and gives the vanishing result when substituted in expressions (37).

The second note is similar to the first one. The formal derivation of the turbulent-viscosity tensor also gives, along with the contributions present in (34), odd contributions with

respect to the angular velocity [73]. They bear no relation to the turbulent dissipation but generate a large-scale flow: the nonuniform rotation gives rise to a meridional circulation and, conversely, the meridional flow generates nonuniform rotation [76]. This closely resembles the $\boldsymbol{\Omega} \times \mathbf{J}$ effect of generating magnetic fields [77], which can also be obtained by formally deriving the tensor of the turbulent diffusion of the magnetic field. Contributions odd in $\boldsymbol{\Omega}$ present in the effective-viscosity tensor can be of interest for the mean-field fluid mechanics and, possibly, can even result in the self-excitation of global flows in rotating fluid bodies. This possibility has not yet been adequately explored. However, it does not seem to be significant for the problem of differential rotation, which deals with more important factors maintaining the differential rotation and meridional flow.

4.4 Effective thermal conductivities

Effective thermal diffusivities (18)–(20) were calculated for a rotating turbulent medium in Ref. [73]. The structure of tensor (18) indicates that in a rotating medium, the eddy thermal diffusivity χ_{\parallel} for the direction along the rotational axis is larger than the corresponding transport coefficient χ_{\perp} for directions transverse to this axis:

$$\chi_{\perp} = \chi_T \phi(\Omega^*), \quad \chi_{\parallel} = \chi_T (\phi(\Omega^*) + \phi_{\parallel}(\Omega^*)). \quad (38)$$

The dependences on Coriolis number (25) shown in Fig. 9 indicate that in the case of fast rotation, the thermal diffusivities for the two directions differ by a factor of two.

The transport coefficient χ_T for a nonrotating medium depends on the deviation from the adiabatic stratification:

$$\chi_T = -\frac{\tau \ell^2 g}{12 c_p} \frac{\partial S}{\partial r}. \quad (39)$$

Therefore, Eqn (16) for the specific entropy is nonlinear.

The equations for large-scale (averaged) fields given in Section 3 together with the Λ -effect and turbulent transport coefficients discussed in this section form a suitable basis for developing quantitative models of differential rotation. We now turn to discussing these models.

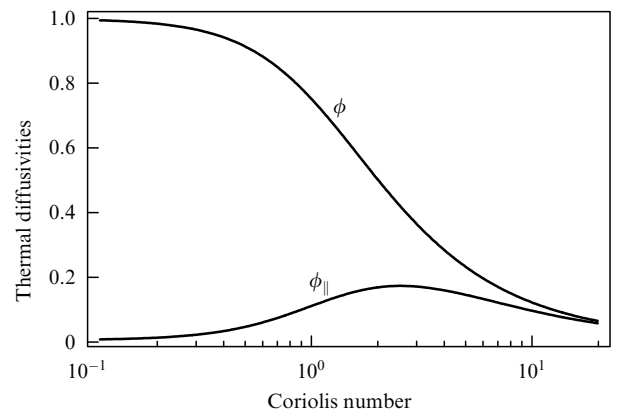


Figure 9. Relative thermal diffusivities (18) and (38) as functions of the Coriolis number (as calculated in Ref. [73]). The thermal conduction is isotropic if rotation is slow. In the case of fast rotation, the heat conductivity along the rotational axis is twice as large as for the directions normal to this axis.

5. The models

5.1 Preliminaries

The scheme in Fig. 10 outlines the formation mechanism for differential rotation in the convective envelopes of stars. The processes represented by the scheme were discussed in Section 3. Evidently, the differential rotation can in principle depend on other factors, which are not reflected by Fig. 10, but none of them has any considerable influence. The inclusion of minor effects in the model seems to contradict the sense of modeling.

At the same time, none of the elements can be removed from the scheme in Fig. 10 without an appreciable effect on the result. This is confirmed by the history of developing the models of differential rotation; in this section, we present this history briefly and without any pretence to completeness.

Kippenhahn's idea [36] that a radial angular-momentum flux (radial A -effect) is sufficient to produce the latitudinal nonuniformity of rotation actually observed on the Sun stimulated a series of studies and led eventually to the development of a quantitative model [78]. It did not take the thermodynamic effects shown in the right-hand part of Fig. 10 into account. The radial A -effect, which was then considered as the anisotropy of eddy viscosity, resulted in a radial nonuniformity of angular velocity. In turn, this nonuniformity inevitably gives rise to a meridional circulation, because the centrifugal force is not potential. The back reaction of the meridional flow on the rotation renders it latitudinally nonuniform. It was found that the relatively fast rotation of the equator requires an anisotropic turbulence in which the horizontal velocities are larger than the radial velocities. The drawbacks of purely hydrodynamic models had then already been evident: at the large Taylor numbers typical of the Sun, the differential rotation is less than the observed one and the isorotational surfaces are cylinders. Such a rotational state contradicts helioseismological data, which, however, were then not yet known. Furthermore, the calculated meridional circulation at the surface is directed from the poles to the equator (oppositely to the observed flow) [49].

Differential rotation can even be obtained without the A -effect, through the baroclinic meridional circulation only. This means that the processes in the left-hand part of Fig. 10 are ignored. The first model of this sort was presented by Durney and Roxburg [79]; subsequently, a similar approach was developed by Belvedere et al. [80, 81]. In such models, the differential temperature resulting from the latitudinal depen-

dence of radial thermal diffusivity (19) was taken into account, while nondiagonal components (20) were neglected. Such models were able to account for the magnitude of differential rotation actually observed on the Sun; however, this required, first, a differential temperature exceeding the maximum value ~ 5 K obtained from observations and, second, a meridional flow directed (at the surface) from the poles to the equator. Furthermore, as is clear today, the distribution of angular velocity did not agree with helioseismological data.

It became gradually apparent that constructing realistic models requires the inclusion of both the A -effect and thermodynamic contributions [82–84]. Only such models can satisfy all observational constraints. However, another difficulty emerges in this case. The characteristics of turbulence, discussed in Section 4, that are necessary to develop models were not known. For this reason, they were introduced as free parameters. Their number was large, and it remained unclear whether agreement between the calculated and observed patterns was a real achievement or the result of a skilled parameter tuning. After the arbitrariness was removed, thanks to the development of the theory of turbulent effects (see Section 4), the models surprisingly proved to be even more successful. Not only did they manage to reproduce the helioseismological data for the Sun but they also made predictions for stars, which gained them some observational support.

To make the picture complete, we note that the development of the theory of the A -effect for arbitrary rotational rates opened up possibilities for the construction of very simple models that include neither the meridional circulation nor the anisotropy of turbulent heat transfer. The latitudinal inhomogeneity of rotation results in this case from the meridional flux of angular momentum, which is nonlinear in Ω^* , Eqns (29). Such models [35, 71] yielded reasonably good results for the Sun, but their predictions for stars turned out to be completely wrong (see, e.g., Ref [85]). The models based solely on the Reynolds stresses are obviously inconsistent: they neglect the meridional flow, which must accompany the differential rotation obtained in these models.

5.2 Mean-field models

In this section, we formulate the models of differential rotation based on mean-field fluid mechanics, which was discussed in Sections 3 and 4. These models contain virtually no free parameters. There are, however, some input parameters that specify the particular star for which the differential rotation is to be computed.

Although the design of such models can be considered a ‘technical detail’, we briefly discuss it here to clarify the basic assumptions that are certainly present in the models.

5.2.1 Original atmosphere. The surface layers of a star are strongly inhomogeneous, which raises computational difficulties. For this reason, it is the practice to exclude a thin spherical surface layer from consideration and place the outer boundary of the calculation region at some relative distance $x_e = r_e/R < 1$.

It is assumed that the star is nearly spherical, i.e., the centrifugal force is small compared to the gravitational force, and hence the rotation has little effect on the structure of the star. The density ρ_e and temperature T_e at the outer boundary $r = r_e$, which are needed for calculations, should be taken from an appropriate model of the internal structure of the

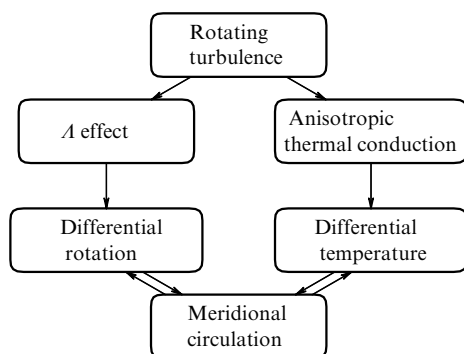


Figure 10. Schematic of the formation of differential rotation in the rotating convective envelope of a star.

star [86]. As mentioned in Section 3, the stratification in stellar convection zones is nearly adiabatic. Therefore, the adiabatic stratification is a good approximation of the distribution of thermodynamic parameters (and the modeling includes the computation of small deviations from this distribution); thus, in view of the hydrostatic equilibrium, the stratification is described as

$$\frac{dT}{dr} = -\frac{g(r)}{c_p}, \quad \frac{dg}{dr} = -2\frac{g}{r} + 4\pi G\rho, \quad \rho = \rho_e \left(\frac{T}{T_e}\right)^{1/(\gamma-1)}, \quad (40)$$

where γ is the adiabatic exponent and G is the gravitational constant.

Equations (40) are (numerically) integrated from the upper boundary of the modeled region to the distance $x_i = r_i/R$, where the radiative heat flux

$$\mathbf{F}^{\text{rad}} = -\frac{16\sigma T^3}{3\kappa\rho} \nabla T \quad (41)$$

is equal to the luminosity of the star L , i.e., $F^{\text{rad}} = L/(4\pi r_i^2)$. This distance corresponds to the base of the convection zone; it is also the lower boundary of the modeled region. Even below, a radiative, stably stratified zone is located, in which no turbulence is present. Here, immediately under the base of the convective layer, the so-called tachocline is located; this is a thin layer in which a transition from the differential to a uniform rotation takes place. We discuss it separately.

The opacity κ that appears in Eqn (41) for the convection zones of solar-type stars is described satisfactorily by the Kramers formula $\kappa = c_\kappa \rho T^{-7/2}$, where c_κ depends on the chemical composition (for the Sun, $c_\kappa = 2.04 \times 10^{24}$ CGS units). In practice, x_i is also taken from the internal-structure models for the stars, and the corresponding c_κ value is adjusted so as to match the computed x_i to its given value.

5.2.2 Original turbulence. The transport coefficients for the original turbulence can be expressed via Eqn (26) in terms of the actual deviation of the medium from the adiabatic stratification:

$$v_T = -\frac{\tau \ell^2 g}{15c_p} \frac{\partial S}{\partial r}, \quad \chi_T = \frac{5v_T}{4}. \quad (42)$$

The distribution of the entropy S should be determined from the system of equations of the model, and hence the equations with transport coefficients (42) are nonlinear.

The mixing length ℓ is assumed to be proportional to the scale height,

$$\ell = \alpha_{\text{MLT}} H_p = \frac{\alpha_{\text{MLT}} P}{\rho g}. \quad (43)$$

The proportionality coefficient α_{MLT} is, as a rule, the only free parameter (we specially stipulate the situations where this is not the case). As we see in what follows, the results are weakly sensitive to variations in this parameter.

The mixing time τ for the nonrotating medium can be found from the solution S_0 of the steady-state version of Eqn (16) with isotropic thermal conduction, in which the contribution of meridional circulation vanishes in the absence of rotation:

$$\tau = \left(-\frac{g}{4c_p} \frac{\partial S_0}{\partial r} \right)^{-1/2}. \quad (44)$$

The time τ is assumed to be independent of the rotational velocity. Therefore, calculations based on formula (44) can be used in the definition of Coriolis number (25), where Ω is the local velocity of nonuniform rotation. In the resulting expressions, all transport coefficients are in a complex dependence on this velocity [see, e.g., Eqn (32)], which adds to the nonlinearity of the equations of the model. The assumption that the mixing time is independent of the rotational velocity is, in all likelihood, fairly crude but cannot be avoided.

5.2.3 System of equations, boundary conditions, and input parameters. The model determines the distributions of angular velocity, meridional circulation, and specific entropy over the convective envelope of the star by numerical solution of the system of steady-state equations (9), (13), and (16) with the Reynolds stresses and eddy heat conductivities found in Section 4.

The boundary conditions for the large-scale flow dictate that Reynolds stresses (7) vanish,

$$R_{\phi r} = R_{\theta r} = 0, \quad (45)$$

at the upper (r_e) and lower (r_i) boundaries. Condition (45) means that no external surface forces are present. In addition, ‘closed’ boundaries are considered, i.e., the radial component of the mean velocity vanishes at the boundaries.

We assume the heat flux at the lower boundary to be time- and latitude-independent, $F_r = L/(4\pi r_i^2)$, and assume the black-body emission of the outer boundary. Some complications result from the fact that the upper boundary of the simulation region is somewhat lower than the surface of the star. Therefore, we need the additional assumption that the thin layer $r_e < r < R$ is a perfect heat exchanger, i.e., its effective heat conductivity is very high, such that all entropy perturbations (with the unperturbed entropy put to zero now) at the base of this layer show up at the emitting surface without any distortions [29]. Then the following condition is satisfied at $r = r_e$:

$$F_r = \frac{L}{4\pi r_e^2} \left(1 + \frac{TS}{c_p T_{\text{eff}}} \right)^4, \quad (46)$$

where $T_{\text{eff}} = (L/(4\pi\sigma R^2))^{1/4}$ is the effective temperature of the star.

For the Λ -effect, we consider only its most important component (33) associated with density inhomogeneities, neglecting anisotropy contribution (30). This approximation reduces the number of free parameters but can introduce some errors, which we discuss in Section 6.1.

We do not dwell on the numerical techniques employed to solve the equations. We only note that the boundary layers (see the closing part of Section 3.2) require a high spatial resolution in the radial direction. Attempts to eliminate these layers, e.g., by including their influence in somehow modified boundary conditions, have yielded no results.

The model requires specifying the following nine parameters: the radius R , luminosity L , and mass M of the star; its mean rotational velocity Ω_0 ; the relative radii of the base of the convection zone, x_i , and of the upper boundary of the simulation region, x_e ; the density ρ_e and temperature T_e at the upper boundary; and the parameter of the mixing-length theory, α_{MLT} . The number of parameters is large, but some freedom of choice is only associated with α_{MLT} . The other

quantities are input parameters rather than free parameters, because they specify the star for which the differential rotation is to be computed.

5.2.4 Estimate for the expected differential rotation. The expected differential rotation can be estimated using the equation of meridional flow (13). For large Taylor numbers (15), the left-hand side of Eqn (13) is small compared to any term on the right-hand side. In the bulk of the convection zone, the two contributions on the right-hand side balance each other, i.e., the Taylor–Proudman balance occurs. We estimate the nonuniformity of the angular velocity in the axial direction to be $\partial\Omega/\partial z \sim \Delta\Omega/R$ and find

$$\frac{\Delta\Omega}{\Omega} \sim \frac{g\nabla S}{\Omega^2 c_p} \sim \frac{\langle u^2 \rangle^\circ}{\ell^2 \Omega^2 \sqrt{\phi(\Omega^*)}}, \quad (47)$$

where the relative thermal diffusivity $\phi(\Omega^*)$ at large Coriolis numbers behaves as $\phi \simeq 1/\Omega^*$. This leads us to the estimate

$$\frac{\Delta\Omega}{\Omega} \sim \frac{4}{\Omega^{*3/2}}. \quad (48)$$

Numerical calculations agree reasonably well with estimate (48) for rotational velocities close to the solar value, but $\Delta\Omega/\Omega$ at larger velocities decreases with Ω^* more slowly than Eqn (48) predicts. This is possibly the effect of boundary layers, in which the Taylor–Proudman balance fails.

Nevertheless, estimate (48) leads to two important conclusions, which are confirmed, at least qualitatively, by both model calculations and observations of the differential rotation of stars.

(1) Given the spectral class of the star [given τ , see Eqn (44)], the absolute magnitude of the differential rotation $\Delta\Omega$ depends weakly on the rotational velocity.

(2) Given the angular velocity Ω , stars of later spectral classes (of smaller masses) rotate more uniformly.

The second conclusion follows from the increase in the mixing time τ with the decrease in the mass of the star [86].

5.2.5 The tachocline. The lower boundary of the above-described model of differential rotation is the base of the convection zone. The so-called tachocline is located below it — a thin layer in which the transition from differential to uniform rotation occurs (see Fig. 2). The processes that produce the tachocline bear no direct relation to the differential rotation of the convection zone, and the transition layer should be considered separately.

Various hypotheses on the origin of the tachocline have been put forward. The results discussed below were obtained using a model in which the relic magnetic field of the radiative zone is responsible for the formation of the transition layer [87–89]. One cannot be completely confident that this model is correct, but it currently offers the only approach that allows obtaining the tachocline from a solution of MHD equations. A relic field with a strength as small as 10^{-3} G is sufficient to produce a tachocline [87]. Its presence cannot notably affect the formation of differential rotation in the convection zone of the star. The nonuniform rotation is calculated using the above-described model independently of the calculations of the transition layer, but the results provide a boundary condition for the model of the tachocline in the form of the angular-velocity distribution at the lower boundary of the convection zone [90].

Other hypotheses for the origin of the tachocline, which do not assume the presence of a relic magnetic field, have also been expressed [91–94]. In one way or another, they consider the instability of differential rotation in the radiative zone, which is believed to destroy the nonuniformity of rotation. The basic difficulty of such approaches arises from the fact that the instability sets in as the differential rotation exceeds a certain threshold value. The development of instabilities normally brings unstable systems to threshold states associated with these instabilities. Therefore, the instability of a uniformly rotating radiative zone could reduce the magnitude of the differential rotation but should not completely remove it.

5.3 Findings of mean-field models

5.3.1 The Sun. The input parameters for the ‘standard’ model of the differential rotation of the Sun are given in Table 2 in the next section. We recall that the latitude-averaged angular velocity of the Sun is $\Omega_0 = 2.87 \times 10^{-6}$ rad s $^{-1}$. The theory of the internal structure of stars yields its best results if $1.5 < \alpha_{\text{MLT}} < 2$ [86]. Below, unless otherwise specified, we discuss calculations for $\alpha_{\text{MLT}} = 1.7$.

The computed distribution of the angular velocity is shown in Fig. 11. By and large, these results agree with helioseismological data on the internal rotation of the Sun [7, 8] (see Fig. 2). Throughout the volume of the convection zone, a so-called equatorial acceleration is present: the angular velocity increases from the poles to the equator, somewhat decreasing with the depth. A thin layer of transition from differential to solid-body rotation is located under the convection zone. In the bulk of the radiative zone, the rotation is virtually uniform. In essence, the computed surface rotation mimics the pattern obtained from Doppler measurements (see Fig. 1).

Some discrepancies between the model calculations and observational data can be found near the outer surface. They are especially pronounced in the computed meridional circulation shown in Fig. 12. It is noteworthy that the direction of meridional circulations changes at small depths, such that the surface flow is directed toward the equator. Observations reveal a poleward flow [49].

These discrepancies can occur because the A -effect included in the model results exclusively from the inhomogeneity of density. The contribution of the anisotropy of turbulence was neglected. It can be seen from a comparison between Figs 6 and 7 that the contributions of anisotropy are small at large Coriolis numbers. The depth dependence of the

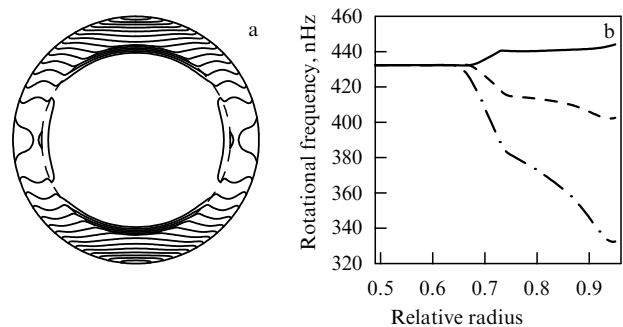


Figure 11. (a) Computed contours of angular velocity. (b) Depth dependences of the angular velocity at the equator (solid curve), at the latitude 45° (dashed curve), and at the poles (dot-dashed curve).

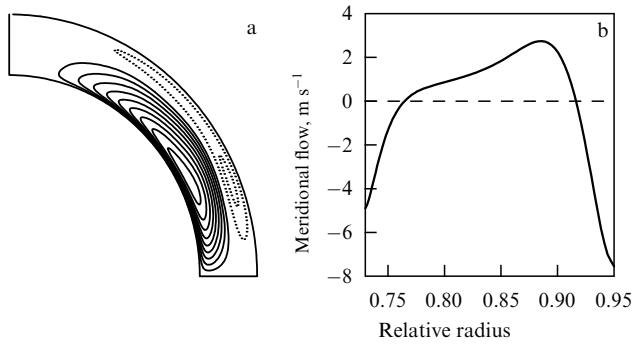


Figure 12. (a) Streamlines of the meridional flow and (b) the radial dependence of the meridional velocity at the latitude 45°. Negative velocity values correspond to equatorward flow. Counterclockwise circulation is shown by solid streamlines and clockwise circulation by dashed streamlines.

Coriolis number in the solar convection zone is shown in Fig. 13. This number is substantially larger than unity deep inside the Sun, and the anisotropy has no effect there. Near the surface, however, $\Omega^* \sim 1$, and the anisotropy may be significant.

Recent calculations have shown that taking the anisotropy into account can actually improve the agreement with observations. If the radial velocities in the original turbulence are about 10% larger than the horizontal velocities, one meridional-circulation cell develops in which the flow is directed poleward near the surface and equatorward at the base of the convection zone. However, as noted in Section 4.2, the inclusion of anisotropy adds a free parameter. Mean-field models are based on the quasilinear theory of turbulent effects and are not highly accurate. The removal of fine distinctions from observations can hardly compensate the arbitrariness that results from the use of the additional free parameter.

We note that the case of fast rotation ($\Omega^* \gg 1$), where the anisotropy plays no part, is most interesting in calculations of the differential rotation. All the results that are discussed below were obtained for the \mathcal{A} -effect determined solely by inhomogeneity. In this case, only the parameter α_{MLT} can be varied and only within a relatively narrow range. The point is that this parameter is also used in the theory of the internal structure of stars, where it has a pronounced effect on the

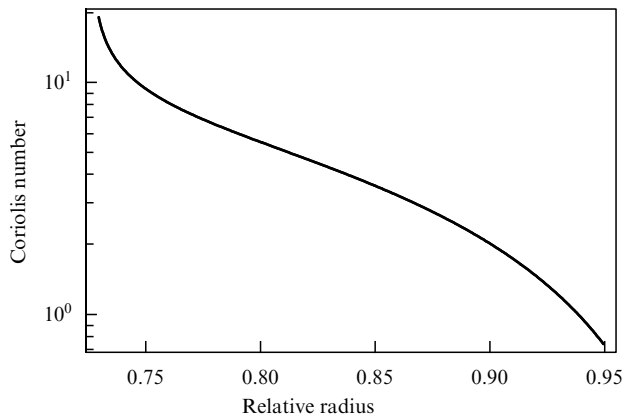


Figure 13. The Coriolis number $2\tau\Omega_0$ as a function of depth in the solar convection zone.

computed radius of the star [13, 86], and satisfactory results can only be obtained if it lies within the range indicated in Table 1. As can be seen from this table, the results of model calculations depend weakly on α_{MLT} . We note that the calculated differential temperature is within the limits imposed by observations. In the models, the temperature at the poles is higher than at the equator.

Table 1. Dependence on α_{MLT} .

α_{MLT}	1.4	1.7	2.0	2.3
$\Delta\Omega/\Omega$	0.30	0.26	0.23	0.21
$\Delta T, \text{K}$	5.7	4.5	3.6	3.0

5.3.2 Solar-type stars. The parameters of solar-type stars of the main sequence for which the differential rotation was calculated are given in Table 2. It is the Sun that is meant by the G2 star. It seems interesting to compute the differential rotation for the infant Sun, which rotated much faster than today. In these computations, we do not take variations in the chemical composition of the star with its age into account. The second star has a relatively small mass and belongs to spectral class K5.

Table 2. Parameters of main-sequence stars.

Star	M/M_\odot	L/L_\odot	R/R_\odot	x_i	x_e	$\rho_e, \text{g cm}^{-3}$	T_e, K
G2	1	1	1	0.73	0.95	7.46×10^{-3}	2.86×10^5
K5	0.7	0.133	0.644	0.69	0.95	6.77×10^{-2}	3.43×10^5

Observations determine only the surface differential rotation of stars. The calculated functions of the rotational period are shown in Fig. 14. Other calculated parameters can be found in Refs [24, 25]. For a fixed spectral class, the absolute magnitude of differential rotation is virtually constant in the range of sufficiently short periods. There is, however, a significant stellar-mass dependence, which, as noted in Section 5.2, may be due to the relatively slow convection in later-spectral-class stars.

The boundary layers discussed in Section 5.3 become important for rapidly rotating stars. An example is presented in Fig. 15, which shows that the meridional flow is concentrated in thin layers near the boundaries of the convection

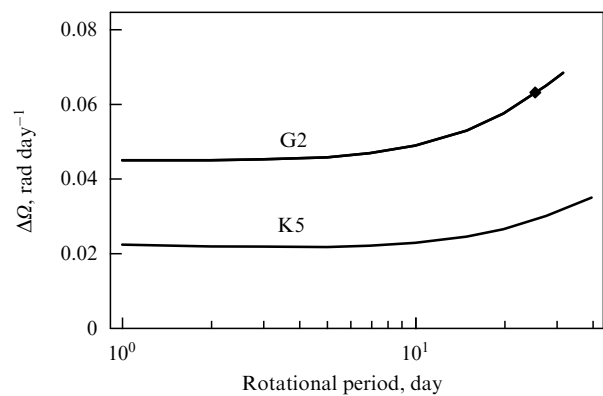


Figure 14. Calculated rotational-period dependences of the equator – pole difference of angular velocities $\Delta\Omega = \Omega_{\text{eq}} - \Omega_{\text{pole}}$ for main-sequence dwarfs. The black square marks the result for the Sun.

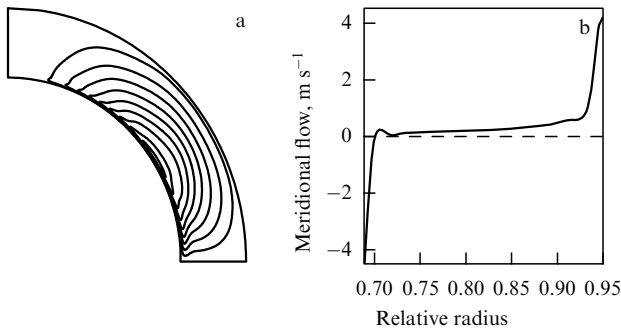


Figure 15. (a) Streamlines of meridional circulation and (b) its velocity at the latitude 45° as a function of the radius for a K5 star with the rotational period 10 days. The meridional flow is concentrated in thin layers near the boundaries of the convective envelope, where the Taylor–Proudman balance fails.

zone. The boundary layers are more pronounced in stars of later spectral classes, because Taylor number (15) estimated to be $Ta \simeq 10\Omega^{*2}(R/\ell)^4$ [25] is larger for later spectral classes, given the rotational period.

The theoretical predictions agree reasonably well with recent Doppler-imaging determinations of differential rotation for K and G stars (see Fig. 4 and Ref. [23]). The enhancement of the rotational nonuniformity with the mass of the star appears to continue for F stars [95, 96].

There are, however, contradictions with earlier determinations of the angular-velocity dependence of the differential rotation based on a long series of photometric observations [97, 98]. The obtained dependences were approximated by the power law $\Delta\Omega \sim \Omega^n$. This yielded $n \simeq 0.15$ [97] and $n \simeq 0.7$ [98], while the computed dependences (Fig. 14) corresponded to $n \simeq 0$. As noted in Ref. [99], this discrepancy can result from the fact that the determinations of differential rotation were based on large groups of stars without selection according to their spectral classes. Mainly, the relatively long rotational periods appertained to K stars and the shortest periods to F stars. If so, the observationally found dependence passes from the lower curve in Fig. 14 (for longer periods) to the upper curve (for shorter periods). Obviously, this overstates the exponent n .

5.3.3 Giants. Another class of stars to which the theory of differential rotation can be applied is giants of luminosity class III, or ‘normal’ giants. Such stars are several times as massive as the Sun and exceed it in luminosity by a factor of several dozen. They have already completed their residence at the main sequence. During the subsequent evolution, the normal giants acquire outer convection zones and become similar to the above-discussed dwarfs in their structure.

Some very interesting properties of normal giants prompt the calculation of their differential rotation. The rotational velocity of these stars is an unambiguous function of their spectral class [100],

$$u_{\text{eq}} = 7.31 - 0.417 \text{ Sp}, \quad (49)$$

where u_{eq} is the rotational velocity at the equator in km s⁻¹ and Sp is the spectral parameter equal to 3 for spectral class G3, 4 for G4, 10 for K0, etc. (there are, however, examples of

normal giants rotating much more rapidly than formula (49) prescribes) [101, 102]. The spectral class varies with the age of the star, and therefore formula (49) can be considered a relationship between the rotational rate and age. This relationship is possibly controlled by the magnetic activity [103]. At least some normal giants exhibit magnetic-activity cycles of the duration about 10 yr [104]. As on the Sun, spots appear on the normal giants mainly at near-equatorial latitudes [103, 105].

Giants are large in size and rotate slowly, but they are similar to the Sun in dimensionless values of their parameters [25]. In terms of some characteristics, they correspond much more closely to the solar type than the young, rapidly rotating main-sequence dwarfs do.

The input parameters for the simulation of differential rotation are given in Table 3. Particular rows of the table refer to different evolutionary stages of the same star and represent model data [106]. The calculations were carried out for the evolutionary stages at which magnetic activity is observed for the stars of the considered type.

Table 3. Parameters of an evolving star with a mass of $2.5M_\odot$.

T_{eff} , K	R/R_\odot	x_i	ρ_e , g cm ⁻³	T_e , K	Ω_0 , rad s ⁻¹
5413	7.96	0.69	2.56×10^{-5}	7.94×10^4	1.17×10^{-6}
5236	7.91	0.61	5.69×10^{-5}	8.07×10^4	1.07×10^{-6}
5016	8.88	0.47	6.75×10^{-5}	7.23×10^4	7.48×10^{-7}
4900	10.3	0.36	4.40×10^{-5}	6.00×10^4	4.98×10^{-7}
4794	12.1	0.27	2.83×10^{-5}	5.14×10^4	3.63×10^{-7}
4689	14.6	0.177	1.38×10^{-5}	3.93×10^4	2.73×10^{-7}

The relative magnitudes of the computed differential rotation [25] are shown in Fig. 16. They are close to the magnitudes of the observed rotational inhomogeneity of the Sun. This might explain why the magnetic activity of luminosity-class-III giants is similar to the solar magnetic activity. Unfortunately, observations have not yielded information on the differential rotation of normal giants. Only particular data for stars with anomalously fast rotation are available. The observational verification of the theoretical predictions encounters difficulties that stem from the very slow rotation of stars of this type.

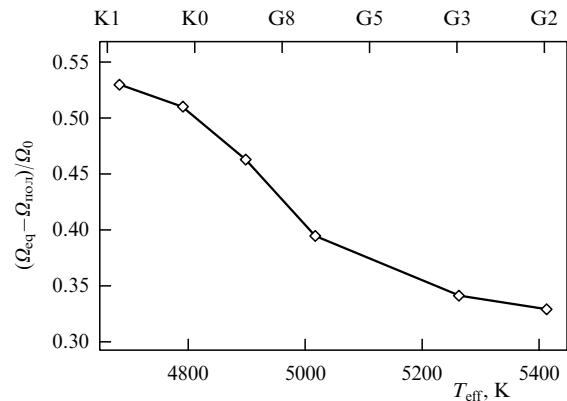


Figure 16. Relative magnitude of the differential rotation at the surface of an evolving giant of mass $2.5M_\odot$. Calculations were done for the sequence of states presented in Table 3. Spectral classes are marked on the upper scale.

5.4 Numerical experiments

So far, we have only discussed models based on the mean-field theory. They determine the global flows on stars from the equations averaged over the ensemble of turbulent flows. These equations contain averaged characteristics of turbulence that can be determined from the quasilinear theory (see Sections 3 and 4). Obviously, an approach with an inverted order of operations is also possible: the equations are solved first and subsequent averaging of the obtained solution determines the large-scale flow. In this case, the solution should be obtained numerically. Numerical calculations of this sort give hope for determining the global flow without a detailed analysis of its origin. For this reason, they have come to be known as numerical experiments. Up to now, numerical experiments have been carried out for only one star, the Sun. It goes without saying that they are not aimed at demonstrating that the Sun obeys the fundamental laws. If the numerical experiments were successful, they would enable us, for example, to determine the convective fluxes of angular momentum, which cannot be directly inferred from observations; thus, our understanding of the nature of differential rotation could be verified.

The first three-dimensional numerical simulations of differential rotation [39, 107] were based on the Boussinesq approximation. Later, the compressibility of the medium was taken into account in the inelastic approximation [41, 108, 109]. The computed magnitude of the differential rotation was comparable to the actually measured solar value, but the distribution of the angular velocity over the convection zone was, as clarified by helioseismology, far from realistic. The angular velocity of the simulated differential rotation was almost constant over rotationally coaxial cylindrical surfaces. Recent numerical experiments [48, 110, 111] were somewhat more successful.

The failure of the numerical experiments is not completely understood. They are probably related to insufficient spatial resolution. The Reynolds numbers must be sufficiently large to 'switch on' the mechanisms of turbulent transport. Of course, we do not mean the actual Reynolds numbers, which are obviously unreachable in numerical experiments; these numbers must merely be large enough for the transport processes to be controlled by turbulent mixing rather than by the prescribed microscopic diffusion coefficients. To all appearances, the opposite situation is typical of numerical computations: the work of the buoyancy force for various convection modes is mainly balanced by dissipative losses, while the nonlinear interaction between modes is weak (see, e.g., Fig. 5 in Ref. [41]). The problem of spatial resolution presents the most severe difficulties near the surface, where small-scale convection occurs. For this reason, the microscopic viscosity is frequently assumed to increase toward the surface, for example, to be inversely proportional to the density of the medium [48]. To a certain extent, this diminishes the difficulties, but it becomes unclear whether the surface layer remains convectively unstable or becomes the region of penetrative convection.

Apparently, only the advent of higher-performance computers can give numerical experiments some chance of success.

6. Prospects

To all appearances, the theory of differential rotation has reached a certain degree of completeness. The basic mechan-

isms that give rise to nonuniform rotation have been studied in detail by the mean-field fluid mechanics of rotating turbulent media [52, 69]. The quantitative models based on this theory agree reasonably well with the observed rotation of the Sun and similar stars. Nevertheless, astronomical observations provide new data, and not all observed phenomena can yet be explained theoretically.

First of all, this refers to time variations in the differential rotation. So-called torsional oscillations of the Sun — periodic 11-yr variations in its rotation — have been known for many years [112, 113]. However, data on the distribution of torsional oscillations in the depths of the Sun [114] were accumulated very recently. Information on torsional oscillations in stars is being acquired [115, 116]. The development of the theory of torsional oscillations is mainly retarded by the lack of adequate models of stellar magnetic fields. Periodic changes in the rotation are most likely related to cyclic variations in the magnetic field. It remains unclear, however, whether these changes result from direct influences of magnetic forces on the large-scale flows or are due to the effect of magnetic forces on the convective fluxes of angular momentum, which form the differential rotation [117]. Resolving this issue would also be important for comprehending the nature of variations in the solar cyclicity on time scales of hundreds of years and longer [118].

The above-discussed theory describes only one type of differential rotation, with the angular velocity growing from the poles to the equator. Differential rotation of this sort is observed on the Sun and on most stars for which it has been successfully measured. There are exceptions, however. About ten stars with so-called antisolar rotation, i.e., with the angular velocity increasing with latitude, are already known [10]. Such rotational states can result from a rapid meridional flow. If the Reynolds number for the meridional circulation is large, the angular-momentum density varies weakly along the streamlines. Therefore, the angular velocity increases with the latitude along these lines. Fast meridional circulation can be expected in the cases where either the gravitational potential or the temperature distribution over the surface of the star deviates significantly from the spherical symmetry [119]. These considerations agree with the observed cases of antisolar rotation, most of which refer to either binary systems or giants with large spots [10]. However, the theory of differential rotation for both binaries and stars whose magnetic fields produce large-scale temperature nonuniformities still remains to be developed.

We note, however, that the theory of differential rotation widely uses the quasilinear approximation of mean-field fluid mechanics. In all likelihood, this is a fairly crude approximation. It is actually surprising that quantitative models based on it agree reasonably well with observations. This agreement does not stimulate the application of more rigorous approaches known in the theory of turbulence (the renormalization technique [58] could be such an approach). Nevertheless, it would be desirable to verify the predictions of the quasilinear theory using numerical simulations. We do not mean the global numerical calculations discussed in Section 5.4, which encounter serious inherent problems. Restricting the numerical calculations of convection to a small part of the rotating convection zone would be sufficient to test the mean-field theory. Such 'local' numerical simulations involve minor difficulties, and some steps forward in this direction have already been made [120–122].

As in most astrophysical theories, progress in the physics of differential rotation depends on observations. It can hardly be imagined how many wrong theoretical studies of solar rotation could appear if helioseismological data were not available. Extending the application of seismological techniques to stars is now in progress. The implementation of astroseismological projects could provide completely unpredictable information.

Acknowledgments. This work was supported by the Russian Foundation for Basic Research (project code 02-02-16044).

References

- Parker E N *Cosmical Magnetic Fields: Their Origin and Their Activity* (Oxford: Clarendon Press, 1979)
- Vainshtein S I, Zel'dovich Ya B, Ruzmaikin A A *Turbulentnoe Dinamo v Astrofizike* (Turbulent Dynamos in Astrophysics) (Moscow: Nauka, 1980)
- Carrington R C *Observations of the Spots on the Sun from November 9, 1853, to March 24, 1861* (London: Williams & Norgate, 1863)
- Sokoloff D D *Solar Phys.* **224** 145 (2004)
- Vorotsov S V, Zharkov V N, in *Itogi Nauki i Tekhniki. Astronomiya* (Progress in Science and Technology: Astronomy) Vol. 38 (Moscow: VINITI, 1988) p. 253
- Gough D O, Thompson M J, in *Solar Interior and Atmosphere* (Eds A N Cox, W C Livingston, M S Matthews) (Tucson: Univ. of Arizona Press, 1991) p. 519
- Schou J et al. *Astrophys. J.* **505** 390 (1998)
- Wilson P R, Burtonclay D, Li Y *Astrophys. J.* **489** 395 (1997)
- Donati J-F, in *Stellar Surface Structure.: Proc. of the 176th Symp. of the IAU, Vienna, Austria, October 9–13, 1995* (Eds K G Strassmeier, J L Linsky) (Dordrecht: Kluwer Acad. Publ., 1996) p. 53
- Strassmeier K G, in *Stars as Suns: Activity, Evolution and Planets* (IAU Symp., Vol. 219, Eds A K Dupree, A O Benz) (San Francisco, CA: Astron. Soc. of the Pacific, 2004) p. 39
- Howard R et al. *Solar Phys.* **83** 321 (1983)
- Newton H W, Nunn M L *Mon. Not. R. Astron. Soc.* **111** 413 (1951)
- Stix M *The Sun: An Introduction* (Berlin: Springer-Verlag, 1989)
- Vogt S S, Penrod G D *Publ. Astron. Soc. Pacific* **95** 565 (1983)
- Khokhlova V L *Astron. Zh.* **52** 950 (1975)
- Khokhlova V L *Astron. Nachr.* **297** 203 (1976)
- Goncharskii A V, Cherepashchuk A M, Yagola A G *Nekorrektnye Zadachi Astrofiziki* (Ill-Posed Problems in Astrophysics) (Moscow: Nauka, 1985)
- Donati J-F, Cameron A C *Mon. Not. R. Astron. Soc.* **291** 1 (1997)
- Petit P, Donati J-F, Cameron A C *Astron. Nachr.* **325** 221 (2004)
- Barnes J R et al. *Mon. Not. R. Astron. Soc.* **314** 162 (2000)
- Donati J-F, Cameron A C, Petit P *Mon. Not. R. Astron. Soc.* **345** 1187 (2003)
- Donati J-F et al. *Mon. Not. R. Astron. Soc.* **316** 699 (2000)
- Barnes J R et al. *Mon. Not. R. Astron. Soc.* **357** L1 (2005)
- Kichatinov L L, Rüdiger G *Pis'ma Astron. Zh.* **23** 838 (1997) [*Astron. Lett.* **23** 731 (1997)]
- Kichatinov L L, Rüdiger G *Astron. Astrophys.* **344** 911 (1999)
- Lebedinskii A I *Astron. Zh.* **18** 10 (1941)
- Monin A S, Yaglom A M *Statisticheskaya Gidromekhanika* (Statistical Fluid Mechanics) (Moscow: Nauka, 1965, 1967) [Translated into English: *Statistical Fluid Mechanics; Mechanics of Turbulence* (Cambridge, Mass.: MIT Press, 1971, 1975)]
- Gough D O *J. Atmos. Sci.* **26** 448 (1969)
- Gilman P A, Glatzmaier G A *Astrophys. J. Suppl. Ser.* **45** 335 (1981)
- Rüdiger G *Geophys. Astrophys. Fluid Dyn.* **16** 239 (1980)
- Ward F *Astrophys. J.* **141** 534 (1965)
- Ribes E *Adv. Space Res.* **6** 221 (1986)
- Komm R W, Howard R F, Harvey J W *Solar Phys.* **151** 15 (1994)
- Nesme-Ribes E, Ferreira E N, Vince L *Astron. Astrophys.* **276** 211 (1993)
- Küker M, Rüdiger G, Kichatinov L L *Astron. Astrophys.* **279** L1 (1993)
- Kippenhahn R *Astrophys. J.* **137** 664 (1963)
- Kichatinov L L, Rüdiger G *Astron. Astrophys.* **299** 446 (1995)
- Greenspan H P *The Theory of Rotating Fluids* (London: Cambridge Univ. Press, 1968)
- Gilman P A *Geophys. Astrophys. Fluid Dyn.* **8** 93 (1977)
- Glatzmaier G A *J. Comput. Phys.* **55** 461 (1984)
- Gilman P A, Miller J *Astrophys. J. Suppl. Ser.* **61** 585 (1986)
- Brandenburg A, Moss D, Tuominen I *Astron. Astrophys.* **265** 328 (1992)
- Brandenburg A et al. *Solar Phys.* **128** 243 (1990)
- Durney B R *Solar Phys.* **123** 197 (1989)
- Kitchatinov L L, Rüdiger G *Pis'ma Astron. Zh.* **21** 216 (1995) [*Astron. Lett.* **21** 191 (1995)]
- Durney B R *Astrophys. J.* **511** 945 (1999)
- Durney B R *Astrophys. J.* **407** 367 (1993)
- Brun A S, Toomre J *Astrophys. J.* **570** 865 (2002)
- Komm R W, Howard R F, Harvey J W *Solar Phys.* **147** 207 (1993)
- Zhao J, Kosovichev A G *Astrophys. J.* **603** 776 (2004)
- Landau L D, Lifshitz E M *Gidrodinamika* (Fluid Mechanics) (Moscow: Nauka, 1988) p. 272 [Translated into English (Oxford: Pergamon Press, 1987)]
- Rüdiger G *Differential Rotation and Stellar Convection* (New York: Gordon and Breach Sci. Publ., 1989)
- Altrock R C, Canfield R C *Solar Phys.* **23** 257 (1972)
- Falciani R, Rigutti M, Roberti G *Solar Phys.* **35** 277 (1974)
- Kuhn J R, Libbrecht K G, Dicke R H *Nature* **328** 326 (1987)
- Pipin V V, Kichatinov L L *Astron. Zh.* **77** 872 (2000) [*Astron. Rep.* **44** 771 (2000)]
- Brandenburg A, in *The Cosmic Dynamo: Proc. of the 157th Symp. of the IAU, Potsdam, Germany, September 7–11, 1992* (Eds F Krause, K-H Rädler, G Rüdiger) (Dordrecht: Kluwer Acad. Publ., 1993) p. 111
- McComb W D *Rep. Prog. Phys.* **58** 1117 (1995)
- Moffatt H K *Magnetic Field Generation in Electrically Conducting Fluids* (Cambridge: Cambridge Univ. Press, 1978) [Translated into Russian (Moscow: Mir, 1980)]
- Durney B R, Spruit H C *Astrophys. J.* **234** 1067 (1979)
- Kichatinov L L *Astron. Astrophys.* **243** 483 (1991)
- Kichatinov L L *Geophys. Astrophys. Fluid Dyn.* **35** 93 (1986)
- Kichatinov L L *Astron. Zh.* **64** 135 (1987) [*Sov. Astron. Rep.* **31** 68 (1987)]
- Schwarzschild M *Structure and Evolution of the Stars* (Princeton: Princeton Univ. Press, 1958) [Translated into Russian (Moscow: IL, 1961)]
- Wasiutynski J *Astrophys. Norvegica* **4** 1 (1946)
- Iroshnikov R S *Astron. Zh.* **46** 97 (1969) [*Sov. Astron. Rep.* **13** 73 (1969)]
- Rüdiger G *Geophys. Astrophys. Fluid Dyn.* **25** 213 (1983)
- Durney B R, Latour J *Geophys. Astrophys. Fluid Dyn.* **9** 241 (1978)
- Rüdiger G, Hollerbach R *The Magnetic Universe* (Weinheim: Wiley-VCH, 2004)
- Kichatinov L L *Pis'ma Astron. Zh.* **12** 410 (1986) [*Sov. Astron. Lett.* **12** 172 (1986)]
- Kichatinov L L, Rüdiger G *Astron. Astrophys.* **276** 96 (1993)
- Kichatinov L L *Geophys. Astrophys. Fluid Dyn.* **38** 273 (1987)
- Kichatinov L L, Pipin V V, Rüdiger G *Astron. Nachr.* **315** 157 (1994)
- Biermann L Z. *Astrophys.* **28** 304 (1951)
- Lifshitz E M, Pitaevskii L P *Fizicheskaya Kinetika* (Physical Kinetics) (Moscow: Nauka, 1979) p. 45 [Translated into English (Oxford: Pergamon Press, 1981)]
- Kichatinov L L, in *Turbulence, Waves and Instabilities in the Solar Plasma* (NATO Sci. Series, Ser. II, Vol. 124, Eds R Erdélyi et al.) (Dordrecht: Kluwer Acad. Publ., 2003) p. 81
- Krause F, Rädler K-H *Mean-Field Magnetohydrodynamics and Dynamo Theory* (Oxford: Pergamon Press, 1980) [Translated into Russian (Moscow: Mir, 1984)]
- Köhler H *Solar Phys.* **13** 3 (1970)
- Durney B R, Roxburg I W *Solar Phys.* **16** 3 (1971)
- Belvedere G, Paternó L *Solar Phys.* **54** 289 (1977)
- Belvedere G, Paternó L, Stix M *Geophys. Astrophys. Fluid Dyn.* **14** 209 (1980)
- Schmidt W *Geophys. Astrophys. Fluid Dyn.* **21** 27 (1982)
- Moss D, Vilhu O *Astron. Astrophys.* **119** 47 (1983)
- Pidatella R M et al *Astron. Astrophys.* **156** 22 (1986)

85. Johns-Krull C M *Astron. Astrophys.* **306** 803 (1996)
86. Kippenhahn R, Weigert A *Stellar Structure and Evolution* (Berlin: Springer-Verlag, 1994)
87. Kitchatinov L L, Rüdiger G *Pis'ma Astron. Zh.* **22** 312 (1996) [*Astron. Lett.* **22** 279 (1996)]
88. Rüdiger G, Kitchatinov L L *Astron. Nachr.* **318** 273 (1997)
89. MacGregor K B, Cyarbonneau P *Astrophys. J.* **519** 911 (1999)
90. Kitchatinov L L *Astron. Zh.* **81** 176 (2004) [*Astron. Rep.* **48** 153 (2004)]
91. Spiegel E A, Zahn J-P *Astron. Astrophys.* **265** 106 (1992)
92. Charbonneau P, Dikpati M, Gilman P A *Astrophys. J.* **526** 523 (1999)
93. Garaud P *Mon. Not. R. Astron. Soc.* **324** 68 (2001)
94. Garaud P *Mon. Not. R. Astron. Soc.* **329** 1 (2002)
95. Reiners A, Shmitt J H M M *Astron. Astrophys.* **393** L77 (2002)
96. Reiners A, Shmitt J H M M *Astron. Astrophys.* **412** 813 (2003)
97. Hall D S, in *The Sun and Cool Stars: Activity, Magnetism, Dynamos: Proc. of Colloq., No. 130 of the IAU, Helsinki, Finland, 17–20 July 1990* (Lecture Notes in Physics, Vol. 380, Eds I Tuominen, D Moss, G Rüdiger) (Berlin: Springer-Verlag, 1991) p. 353
98. Donahue R A, Saar S H, Baliunas S *Astrophys. J.* **466** 384 (1996)
99. Cameron A C et al., in *Cool Stars, Stellar Systems and the Sun: 11th Cambridge Workshop* (Astron. Soc. of the Pacific Conf. Ser., Vol. 223, Eds J Ramon et al.) (San Francisco, CA: Astron. Soc. of the Pacific, 2001) p. 251
100. Gray D F *Astrophys. J.* **347** 1021 (1989)
101. Hackman T, Jetsu L, Tuominen I *Astron. Astrophys.* **374** 171 (2001)
102. Strassmeier K G, Kratzwald L, Weber M *Astron. Astrophys.* **408** 1103 (2003)
103. Gray D F *Publ. Astron. Soc. Pacific* **101** 1126 (1989)
104. Donahue R A, in *Stellar Surface Structure: Proc. of the 176th Symp. of the IAU, Vienna, Austria, October 9–13, 1995* (Eds K G Strassmeier, J L Linsky) (Dordrecht: Kluwer Acad. Publ., 1996) p. 261
105. Gray D F, in *The Sun and Cool Stars: Activity, Magnetism, Dynamos: Proc. of Colloq., No. 130 of the IAU, Helsinki, Finland, 17–20 July 1990* (Lecture Notes in Physics, Vol. 380, Eds I Tuominen, D Moss, G Rüdiger) (Berlin: Springer-Verlag, 1991) p. 336
106. Herwig F et al. *Astron. Astrophys.* **324** L81 (1997)
107. Gilman P A, Miller J *Astrophys. J. Suppl. Ser.* **46** 211 (1981)
108. Glatzmaier G A *Astrophys. J.* **291** 300 (1985)
109. Glatzmaier G A *Geophys. Astrophys. Fluid Dyn.* **31** 137 (1985)
110. Miesch M S et al. *Astrophys. J.* **532** 593 (2000)
111. Elliot J R, Miesch M S, Toomre J *Astrophys. J.* **533** 546 (2000)
112. Howard R, LaBonte B J *Astrophys. J.* **239** L33 (1980)
113. LaBonte B J, Howard R *Solar Phys.* **75** 161 (1982)
114. Vorontsov S V et al. *Science* **296** 101 (2002)
115. Cameron A C, Donati J-F *Mon. Not. R. Astron. Soc.* **329** 23 (2002)
116. Livshits M A, Alekseev I Yu, Katsova M M *Astron. Zh.* **80** 613 (2003) [*Astron. Rep.* **47** 562 (2003)]
117. Kitchatinov L L *Pis'ma Astron. Zh.* **16** 652 (1990) [*Sov. Astron. Lett.* **16** 280 (1990)]
118. Kitchatinov L L, Pipin V V *Astron. Zh.* **75** 913 (1998) [*Astron. Rep.* **42** 808 (1998)]
119. Kitchatinov L L, Rüdiger G *Astron. Nachr.* **325** 496 (2004)
120. Brandenburg A et al. *J. Fluid Mech.* **306** 325 (1996)
121. Brummel N H, Hurlburt N E, Toomre J *Astrophys. J.* **493** 955 (1998)
122. Käpylä P J, Korpi M J, Tuominen I *Astron. Astrophys.* **325** 793 (2004)